Feasibility of a Predictive Model of *Hsp70b*-Activated Gene Therapy Protein Expression during Ultrasound Hyperthermia

by

Christina Elise Silcox

B.S. Biomedical Engineering
Boston University (2000)

M.S. Electrical Engineering and Computer Science
Massachusetts Institute of Technology (2004)

SUBMITTED TO THE HARVARD-MIT PROGRAM IN HEALTH SCIENCES AND TECHNOLOGY IN PARTIAL FULFILLMENT OF THE REQUIREMENTS FOR THE DEGREE OF

DOCTOR OF PHILOSOPHY IN MEDICAL ENGINEERING AND MEDICAL PHYSICS

AT THE
MASSACHUSETTS INSTITUTE OF TECHNOLOGY
June 2014

Signature of Author Signature redacted
Harvard-MIT Program in Health Sciences and Technology
May 19, 2014

Certified by Signature redacted
Stuart K. Calderwood, PhD
Associate Professor of Radiation Oncology, Beth Israel Deaconess Medical Center
Thesis Supervisor

Accepted by Signature redacted
Emery N. Brown, MD, PhD
Director, Harvard-MIT Program in Health Sciences and Technology
Professor of Computational Neuroscience and Health Sciences and Technology

Feasibility of a Predictive Model of *Hsp70b*-Activated Gene Therapy Protein Expression during Ultrasound Hyperthermia

by

Christina Elise Silcox

Submitted to the Harvard-MIT Program in Health Sciences and Technology
on May 19th, 2014 in Partial Fulfillment of the Requirements for the Degree of Doctor of Philosophy in Medical Engineering and Medical Physics

ABSTRACT

Gene therapy has been heralded as a possible approach to a variety of diseases and conditions, ranging from cancer and heart disease to blindness and neurodegenerative diseases. However, progress in gene therapy requires a delivery system that can control when and where the therapeutic proteins will be generated. Our study was performed to determine the feasibility of attaching heat-inducible promoters to genes of interest in order to control activation of the gene *in vivo* via ultrasound-induced hyperthermia monitored by MRI thermometry.

We first demonstrated that gene therapy-mediated gene expression could be spatially and temporally controlled with this method. Further studies were subsequently performed to determine if the activation of a particular heat-inducible gene, *Hsp70b*, could be quantified and predicted *a priori* during hyperthermia, thus allowing advance knowledge of the protein levels over time. Experiments indicated that as the temperature and duration of a hyperthermic shock increased, peak expression levels of *Hsp70b* mRNA also increased until a saturation level was reached. In addition, as the duration of a hyperthermic shock increased, the time during which *Hsp70b* mRNA remained elevated also increased. Most significantly, a correlation was found between total *Hsp70b* mRNA production generated by thermal shock and thermal dose, a predictor of dose often used in hyperthermia therapies.

The relationship found between total *Hsp70b* mRNA production and thermal dose suggests that a real-time predictive model of therapeutic protein dose kinetics after ultrasound-induced hyperthermia for gene therapy is feasible. However, the creation of such a model would require further precision experimentation for which ultrasonically-induced hyperthermia is not suited. A final study was performed and found that *Hsp70b* was not activated by the mechanical stress caused by ultrasound. These results confirm that a predictive model applicable to ultrasonically-induced hyperthermia could be developed using waterbath techniques that will allow tighter control of temperature.

Thesis Supervisor: Stuart K. Calderwood
Title: Associate Professor of Radiation Oncology, Beth Israel Deaconess Medical Center

Acknowledgements

I would like to thank my thesis advisor, Stuart Calderwood, for his patience and support throughout my doctoral work. There were a lot of ups and downs, and he was extraordinarily understanding and supportive of me. His wisdom and compassion has contributed to my growth as a scientist. I thank Nathan McDannold, my co-advisor, for his patience and guidance with the ultrasound and MRI thermometry portion of this thesis and especially his hands-on willingness to help solve technical problems as soon as they popped up.

I would also like to thank my committee chair, Elfar Adalsteinsson, for his encouragement and Kullervo Hynynen for my start in ultrasound and gene therapy research and his mentorship at the beginning of this work.

It has been a great pleasure to work in Dr. Calderwood's lab and I would like to thank everyone who helped me throughout my time there, both current and former members. I would especially like to thank Ketty Chou and Ayesha Murshid for their constant tutoring and guidance, as well as their friendship. It was not easy to teach an engineer how to be a biologist, but they always had time for my questions. In addition, I would like to thank Ron Smith, Rong Zhong and Bangmin Zhu for their help in teaching me various lab techniques.

The members of the Focused Ultrasound Laboratory at Brigham and Women's hospital have been part of my life since my co-op during my undergraduate years. I cannot list all the current and former members who contributed to my growth as a scientist, but I am grateful to them all. In particular, I would like to thank Sham Sokka, Erich Caulfield, Lisa Treat, Jason White, Phillip Alexander, Costas Arvanitis, Muna Aryal, and Mei Chang-Sheng.

I am grateful to have been part of the Harvard-MIT Program in Health Sciences and Technology. The community in general and especially the good folks in E25-519, Cathy Modica, Julie Greenburg, Traci Anderson and Laurie Ward in particular, have kept me sane (or mostly so) throughout this adventure. I would also like to thank my academic advisor Martha Gray.

I thank my friends, both at MIT and elsewhere, for their love and support of me as well as their ability to make me relax and laugh. I also would like to thank my high school biology teacher, Mr. Peters, for never answering a question he thought I should be able to figure out myself.

Finally and most importantly, I thank my family. I dedicate this thesis to my mother and father, who have nurtured my love of science from the beginning and never allowed limitations to be placed on my education, and to my fiancé David Varisco, who has supported and loved me throughout this experience.

Table of Contents

List of Figures

List of Tables

List of Abbreviations

4T1	Breast cancer cell line
A	Adenine nucleotide
AAV	Adeno-associated virus
Ad	Adenovirus
BCA	Bicinchoninic acid
β-gal	β-galactosidase
BSA	Bovine serum albumin
C	Cytosine nucleotide
c	Speed of sound in water
CAP	Cytoplasmic adaptor proteins
cDNA	Complimentary DNA
CMV	Cytomegalovirus
C_T	C_T number (PCR)
DMEM	Dulbecco's modified Eagle's medium
DNA	Deoxyribonucleic acid
DNase	Deoxyribonuclease
DU-145	Human prostate cancer cell line
EDTA	Ethylenediaminetetraacetic acid
FDA	Food and Drug Administration
FUS	Focused Ultrasound
G	Guanine nucleotide
g	Gravitational acceleration
GFP	Green Florescent Protein
GM-CSF	Granulocyte-macrophage colony-stimulating factor
HeLa	Cervical cancer cell line
HS	Heat Shock
HSE	Heat Shock Element
HSF1	Heat Shock Factor 1
HSP	Heat Shock Protein (a family of similar proteins, individually numbered)
Hsp70b	A specific HSP
Hspa7	Official name of Hsp70b
LCA	Leber's congenital amaurosis
Luc	Luciferase

m	Mass
MEK	Methyl ethyl ketone (butanone)
MR	Magnetic Resonance
MRI	Magnetic Resonance Imaging
mRNA	Messenger RNA
NCBI	National Center for Biotechnology Information
NIH	National Institute of Health
p	p-value, probability
$P_{acoustic}$	Acoustic power
PBS	Phosphate-Buffered Saline
PC3	Human prostate cancer cell line
PCR	Polymerase Chain Reaction
$P_{electric}$	Electrical Power
Pfu	Plague-forming unit
Ppm	Parts per million
RF	Radio Frequency
RNA	Ribonucleic acid
RNase	Ribonuclease
Rpm	rotations per minute
rt-PCR	Real-time PCR
SCID	Severe Combined Immunodeficiency
SCID-X1	A SCID varient
sHsp	small HSPs
T	Thymine nucleotide
T1	T1 relaxation time (MRI)
T2	T2 relaxation time (MRI)
t_{43}	Equivalent-minute (thermal) dose
tRNA	Transfer RNA
T-Vec	Talimogene laherparepvec
US	Ultrasound

1 Introduction

1.1 Motivation

Gene therapy has been heralded as a possible cure for a variety of diseases, ranging from cancer and heart disease to blindness and neurodegenerative diseases. However, progress in gene therapy requires a delivery system that can control when and where the therapeutic proteins will be generated. One method by which this can be achieved is by suppressing the production of the therapeutic proteins by attaching additional DNA segments known as heat-shock protein promoters to the therapeutic gene therapy. This promoter ensures that the protein will only be created in areas and times when the treated cells are heated above a target temperature.

This thesis explores the feasibility of achieving spatially and temporally-controlled gene activation via a minimally invasive procedure using focused ultrasound. In addition, it explores if it possible to mathematically model the amount of therapeutic protein that will be produced given a known heating treatment.

1.2 Introduction to Cell Biology

DNA (deoxyribonucleic acid) is the instruction manual for every living thing. It is composed of different strings of four molecules called nucleotide bases: adenine (A), guanine (G), thymine (T), and cytosine (C). However, DNA is just an instruction manual. Proteins are the building materials. Proteins are made by transcribing and translating discrete sequences of DNA called genes.

DNA is a double helix structure composed of sugar-phosphate backbones and nucleotide base rungs. To make a protein, the double helix is unwound by DNA helicase at the appropriate region where the gene for that protein is located. The double helix unwinds at the start of a gene because of sequences of DNA nucleotides known as promoters. RNA polymerase II will transverse the entire helix, but in general only weakly attaches and detaches quickly to move forward. Specific nucleotide sequences known as promoters allow tighter binding, which cause the unwinding of the helix at that point. Some additional factors are also required for transcription: to position the RNA polymerase correctly, to aid it in the unwinding of the DNA helix and to release the polymerase from the promoter region after transcription has begun. These factors are called transcription factors II (TFII) and differentiated as TFIIA, TFIIB, etc. To begin the transcription process, TFIID binds to a TATA sequence (a sequence composed primarily of T and A nucleotides), located about 25 nucleotides from the start of the promoter. The binding of TFIID distorts the DNA around the TATA box region. The other TFIIs assemble around the distortion, along with RNA polymerase II, to form a complete transcription initiation complex.

Once the helix starts to unwind, RNA polymerase II then attaches what is known as complimentary mRNA bases (which differ from DNA bases by the addition of a sugar ribosome) to each nucleotide on one of the exposed DNA strands. The mRNA base adenine attaches to the DNA base thymine, urcil (U) attaches to adenine, cytosine attaches to guanine and guanine attaches to cytosine. Note that there is no mRNA base thymine so the mRNA base urcil replaces it. This process of making mRNA is called

transcription and occurs at the rate of 20 nucleotides per second in eukaryotic cells. The mRNA strand is quickly released after forming to allow the stronger double helix to reform. Note that mRNA exists as a single strand, which differs from the double-stranded DNA. Due to its single-strand nature, mRNA will fold around itself in different configurations as opposed to the characteristic DNA helix.

Once mRNA is made, a second process known as translation produces the protein encoded by a specified gene. Proteins are made of chains of amino acids. In a similar manner to which each DNA base is matched with a complementary RNA base during translation, sets of three RNA bases match with an amino acid. Because there are 64 possible sets of three RNA bases and only 20 amino acids, more than one 3 base set match with the same amino acid. The matching process in translation is more complicated than in transcription. The amino acids do not directly bind to the RNA bases; instead both bind to opposite sides of small adaptor molecules called transfer RNA (tRNA). Each mRNA strand can be translated multiple times, meaning that a single mRNA strand can produce multiple copies of the encoding protein. The stability of different mRNA strands varies widely, from several minutes to several days, but is fairly consistent between the same mRNA sequences. The mechanism by which mRNA decays, stopping further translation, is not understood in detail.

The initiation of translation, the binding together of the amino acids themselves, and the detachment of the protein from the mRNA and the folding of the protein into the correct

shape is complex, not completely understood, and requires many additional molecules and factors that are not within the scope of this paper.

This section is a summary of Chapters 4-6 of the text "Molecular Biology of the Cell" (Alberts et al., 2002).

1.3 Definition of Gene Therapy

Gene therapy is the introduction of exogenous DNA into a cell that then causes the cell to produce a therapeutically beneficial protein. More specifically, the US Food and Drug Administration defined gene therapy in 2006 as "all products that mediate their effects by transcription and/or translation of transferred genetic material, and/or by integrating into the host genome, and that are administered as nucleic acids, plasmids, viruses, such as adenoviral vectors, or genetically engineered micro-organisms, such as bacteria. These products can be used to modify cells *in vivo*, by a direct administration of a gene therapy product to a patient, or by transfer to cells *ex vivo* prior to patient administration."

There are several ways gene therapy can work, as evidenced by the FDA definition. With all these methods, gene therapy can be done directly *in vivo* or cells can be taken out, modified, and replaced. One gene therapy technique involves adding normal genes into cells with missing or mutated copies of that gene. An example of this is Leber congenital amaurosis (LCA), which is a disease that causes progressive blindness. It was found to be caused by mutations in a gene known as RPE65 in the eye's photoreceptor cells. By

inserting a correct version of the gene into those cells, visual acuity improves, as shown during a Phase I clinical trial, visual acuity was improved in all patients (Cideciyan et al., 2009; Jacobson SG et al., 2012).

Another method of gene therapy is the addition of genes to cells that are not normally present to make cells act in a different way. Many of the cancer gene therapy trials use this principle by inserting genes that cause apoptosis into cancer cells (Cross and Burmester, 2006). One example of this methodology is Talimogene laherparepvec (T-Vec), a gene therapy product that produced initial encouraging results from a phase III clinical trial in 2013 (Andtbacka et al., 2013). T-Vec is a combination of the US11 gene and the gene for the GM-CSF cytokine. The US11 gene kills the tumor cells injected with T-Vec while the GM-CSF produced by the second gene initiates an immune response, attracting dendritic cells which subsequently acquire the ability to identify and kill cancer cells that were not exposed to T-Vec originally.

A third way is to figuratively snip out sections of incorrectly coded DNA currently in the cells. This is a relatively smaller area of study. Two recent examples in the early stages of development are the removal of the extra chromosome in trisomy 21, also known as Down's Syndrome (Li et al., 2012) and the use of non-coding small RNAs to "silence" endogenous mutated genes, such as those in Huntington's disease (Zhang and Friedlander, 2011). With this method the genes are not actually removed but instead the genes are blocked from transcription and translation into the aberrant proteins.

1.4 History of Gene Therapy

Gene therapy took off as an area of intense interest in the 1960's. However, the first real example of gene therapy is a 1928 study known as "Griffith's Experiment". Frederick Griffith inserted the DNA of one variant (type III-S) of *Pneumococcus* bacteria into another variant (type III-R), causing this second variant to have some characteristics of the first. This process became known as transformation and was repeated and improved upon through the 1930's (Dawson and Sia, 1931; Alloway, 1932, 1933). That DNA was the agent causing transformation wasn't demonstrated until 1944 (Avery et al., 1944) and repeated by Hershey and Chase in 1952 (Hershey and Chase, 1952). Interestingly, another study in 1952 showed that the DNA transferring the traits was attached to a bacteriophage (Zinder and Lederberg, 1952), which today we understand made the DNA transfer more efficient and also assisted in actually incorporating the foreign DNA into the host's chromosome. Understanding that bacteria can transfer genetic material efficiently and also retain those new genes as the bacteria divides was a major breakthrough in understanding how different species of bacteria are able to quickly gain resistance to the same antibiotic (Wirth et al., 2013). The possibility of inheritable genetic transfer in mammalian cells was demonstrated in 1962 (Szybalska and Szybalska, 1962). In 1968, Sambrook et al. showed that viruses could integrate stably and heritably into the genomes of mammalian cells very efficiently (Sambrook et al., 1968), causing research to begin on the idea of using modified viruses to transport therapeutic genes into defective cells (Friedmann, 1992).

The lack of appropriate tools for advancing the study of gene therapy slowed progress for the next decade, but in 1973 the first direct human gene trial was performed on two patients suffering from urea cycle disorder (Rogers et al., 1973; Terheggen et al., 1975). The experiment was unsuccessful but it was later found that, due to a misunderstanding of the disorder, the particular gene transferred could not have affected the disease (Wirth et al., 2013). In 1980, Martin Cline performed a human gene therapy trial for thalassaemia involving *in vitro* gene therapy on bone marrow cells. Not only was the experiment unsuccessful, it also had scientific, administrative and ethical issues. The high profile fall-out from this experiment caused the NIH to form a Gene Therapy Subcommittee to regulate human gene therapy experiments, but also made gene therapy a highly visible area of study (Friedmann, 1992).

The next high-profile (and NIH-approved) therapeutic clinical trials involving foreign gene transfer to humans were to treat cancer (Rosenberg et al., 1993) and two types of SCID, a severe immunodeficiency disease (Blaese et al., 1995; Bordignon et al., 1995). Despite many unclear and/or disappointing results, gene therapy research increased substantially until 1999. That year, a patient named Jesse Gelsinger died from a massive immune response to treatment during a clinical trial of a gene that would treat a certain type of liver disease (Stolberg, 1999). It is important to note the distinction that his death was the result of the viral vector used to deliver the therapeutic gene, not the therapeutic gene itself. After this incident research slowed in the United States as the FDA halted all clinical trials until additional protections could be put in place. This lead to what is known as the "lost decade" of gene therapy, which consisted of a return to basic research

to better understand of what gene therapy is realistically capable and the concurrent risks (Lewis, 2014). An example included discovering that retrovirus vectors, which incorporate gene therapy into the cell's own DNA, can cause what is known as insertional mutagenesis, causing oncogenes to become active. Several years after the successful SCID-X1 trials in 1995 mentioned above, 5 of the 20 child test subjects developed leukemia for this reason, causing one fatality in 2004 (Romano, 2012).

Meanwhile, China approved the sale of Gendicine™, the first gene-based product for clinical use, in 2003. It then approved the second gene therapy product for clinical use, Oncorine ™, in 2005. Both were for the treatment of particular types of cancer. In 2004, the European Union approved Cerepro©, for the treatment of brain tumors. Cerepro© became the first adenoviral vector to complete a phase III clinical trial (Wirth et al., 2009) and is now in additional late-stage trials. Since then clinical trials have been done on a variety of diseases and conditions, such as LCA (as mentioned above), B-thalassemia (Cavazzana-Calvo et al., 2010), two types of SCID (Aiuti et al., 2009; Hacein-Bey-Abina et al., 2010), Wiskott-Aldrich syndrome (Boztug et al., 2010), advanced heart failure (Jessup et al., 2011) and glioblastoma (Westphal et al., 2013).

The first European Medicines Agency recommendation of a gene therapy product occured in 2012 for Glybera® after a series of unsuccessful applications. Glybera®'s regulatory and approval issues are detailed in an editorial in *Nature* as part of an overall discussion of the challenges faced by gene therapy products (Ylä-Herttuala, 2012). The FDA has yet to approve of any gene therapy products, but the NIH removed some of the

regulations that have slowed clinical approval in late 2013. Scientific American reports UniQure, the company that manufactures Glybera®, is in early talks with the FDA about approval in the U.S and that industry watchers predict the first U.S. approval of a commercial gene treatment as early as 2016.

1.5 Delivery of Gene Therapy

For gene therapy to be effective, the gene must be delivered past both the cell and nuclear membranes into the cell nucleus. Once in the nucleus, the DNA segment can either be incorporated into the cells' own DNA or remain separate in the nuclear material and use promoters to encourage translation by the host cell messenger RNA. Incorporation into the cell DNA is essential for stable expression of a therapeutic gene. If the therapeutic gene remains separate from the host DNA, expression is lost over time as the cell divides. This property can be used to advantage in the treatment of some diseases, such as apoptotic genes for cancer treatment and the induction of angiogenesis (Worgall, 2005).

Gene therapy can be delivered to target cells by both *in vitro* and *in vivo* methods. There are advantages and disadvantages of each method (Culver, 1996). *In vitro* delivery requires obtaining cells from the patient, delivering the gene therapy, and implanting the cells back into the patient. This has the advantages of both high efficiency, defined as the ratio of gene expression to DNA inputted, and selective delivery of the therapeutic gene to the cell types desired to be transfected. The significant limitation to the *in vitro* method is that the target cells must be removable from the body. This generally limits *in vitro*

gene delivery to hematopietic, endothelial, and tumor cells. In contrast, *in vivo* delivery does not require cells to be removed from the body, but the delivery efficiency is generally much lower and the methods developed to increase this efficiency have additional side effects. In addition, selectively transfecting only certain cell types *in vivo* is challenging.

Modified viruses are the most commonly used and most effective vectors, comprising nearly 70% of clinical trials according to the internet database of gene therapy clinical trials worldwide maintained by the Journal of Gene Medicine (http://www.wiley.com/legacy/wileychi/genmed/clinical/). Viral vectors are classified into categories based on the original viral type, such as retrovirus, adenovirus, vaccinia virus and adeno-associated virus.

Retroviruses were the first viruses modified into viral vectors (Guild et al., 1988; Miller, 1992; Miller et al., 1993; Rivière et al., 1995; Robbins and Ghivizzani, 1998). In the construction of the vector the virus is first disabled of its disease function and made incapable of replication. The therapeutic gene desired for transfer is then grafted onto the stripped virus. Different viral vectors have different useful attributes as well as disadvantages. For example, retroviral vectors retain the ability to reverse transcribe into the target cells' DNA, thus have the ability to integrate into the host DNA and allowing the therapeutic gene to divide with the cell (McTaggart and Al-Rubeai, 2002). This property can be advantageously exploited when treating disease states that require

lifelong therapeutic effects but render retroviruses inappropriate for disease states that only need temporary therapy. Other concerns with retroviral vectors involve long-term side effects as well as fears that the virus may mutate back into a replication-capable form or integrate into an oncogene site and promote cancerous growth. This last fear heightened after several children treated with a retrovirus-delivered gene therapy agent developed a leukemia-like disease several years after treatment (Hacein-Bey-Abina et al., 2003).

Adenoviruses are a class of viruses most commonly associated with causing upper respiratory infections but can also cause pharyngitis, conjunctivitis, gastroenteritis and pneumonia. Unlike retroviruses, these vectors do not integrate into the host cell DNA, which causes the therapeutic function to be lost over time. Adenoviruses have the ability to transfect a wide variety of cell types and can transfect non-dividing as well dividing cell types. The smaller size of adenoviral vectors allow delivery in higher titer volumes than retroviruses (10^{12} to 10^{13} viral particles/mL) (Volpers and Kochanek, 2004) and efficiency is high meaning large amounts of therapeutic protein can be produced from a single injection. The biggest concern in using adenoviruses is the danger demonstrated by the highly publicized death of Jesse Gelsinger in September 1999, which was caused by an immune response to administration of the adenoviral vector. Adenoviral vectors express low levels of viral antigens following infection. This often stimulates an immune response to the infected cells and results in a loss of therapeutic gene expression 1–2 weeks after injection (Yang and Wilson, 1995; Yang et al., 1996). In the Gelsinger case, the amount of virus given to him caused such an immense and immediate immune

reaction that several of his organs went into failure. Strict control over dosage and concurrent immunosuppressive therapy can be used to control this side effect but may still ultimately limit adenoviral vector usefulness. So-called "second generation" and "gutless" adenoviruses are currently in development to help solve these problems (Volpers and Kochanek, 2004).

The adeno-associated virus (AAV) is not technically a virus but rather a symbiotic organism found with adenoviruses. Because AAVs are not known to cause any diseases in humans and no immune response is caused by the introduction of AAVs, these vectors are considered very safe. The disadvantages of using AAV vectors are mostly practical: the small size of the vector restricts the size of the therapeutic gene that can be attached to less than 5.2kB and these vectors are very expensive to produce. Also, recent research has found that AAV vectors integrate preferentially into the gene-rich areas of the host chromosomes (Nakai et al., 2003). This means that AAV vectors could potentially share some of the risks now being associated with retroviruses, but since AAV vectors only integrate into cell chromosomes rarely, the risk is much reduced.

Due to ongoing concerns about the safety of viral vectors, non-viral vectors have also been explored, both biological and physical: liposome transport, naked DNA injection, electroporation and ultrasound among others. In the 1990s it was shown that naked plasmid DNA injection can induce gene expression in skeletal muscle (Wolff et al., 1990), liver (Hickman et al., 1994), thyroid (Sikes et al., 1994), heart muscle (Ardehali et

al., 1995), brain (Schwartz et al., 1996), and urological organs (Yoo et al., 1999). Although naked DNA injection usually does not cause integration into the chromosome, expression can persist for several months (Acsadi et al., 1991; Manthorpe et al., 1993). However, transfection efficiencies are much lower than with viral vector. By transporting genes on liposomes, the negative charge of the DNA is decreased, facilitating interactions with cell membranes and increasing transfection efficiency (although not up to viral vector levels). Liposomes also protect the DNA from damage, cause no immunogenic response and can be designed to target specific cells and tissues. Electroporation, the application of short and intense DC electric pulses that can reversibly increase cell membrane permeability (Mir et al., 1988), is an effective tool for delivering gene therapy *in vitro* but is limited *in vivo*. Ultrasound, however, has the advantage of being able to be used in conjunction with other vectors and can also direct the gene therapy to target tissues/cells.

In addition to the requirement that gene therapy be delivered to cells in sufficient quantities, there has also always been interest in the ability to turn therapeutic genes on and off to control the amount of expressed protein and the location in which it is expressed. Indeed, in Rome's 2005 review of the subject, she specified that to be truly useful, the genes would need to be activated in a dose-dependent fashion to ensure precise control of therapeutic gene expression (Rome et al., 2005). The FDA agrees, stating in its 2006 Guidance for Industry: Preclinical Assessment of Investigational Cellular and Gene Therapy Products that "[w]hile persistent transgene expression may be a desired endpoint for some [Gene Therapy] products, it can also be an undesired

outcome for other products due to overexpression, accumulation of transgene protein, or the risk of an abnormal immune response. Prolonged expression of transgenes such as growth factors, growth factor receptors, or immune-modulating agents, may be associated with long-term risks due to unregulated cell growth, malignant transformation, autoimmune reactions to self-antigens, altered expression of the host's genes, or other unanticipated adverse effects."

1.6 Introduction to Ultrasound

There are several methods that could theoretically be used to heat and activate a gene therapy construct using an heat-activated promoter such as x-rays, lasers, radiofrequency (RF) waves or ultrasound. However, ultrasound is the most logical choice. X-rays have radiation side-effects which limit their usefulness. Lasers can only penetrate millimeters into the skin. RF and ultrasound both can go deeper into the body, but ultrasound can penetrate deeper while remaining tightly focused on a particular spot (Moonen, 2007).

Ultrasound is a form of mechanical energy that exists as an oscillating pressure wave with frequencies between 20kHz and 20MHz. It travels at a speed of approximately 1550 m/s in soft tissues, 1480 m/s in fatty tissues and 343 m/s in air. Ultrasound has been known to bring about changes in tissue structure and biological processes if given in high enough intensities since the 1920s (Harvey, EN, 1928; Wood, RW and Loomis, AL, 1927). Early investigations suggested the possibility of ultrasound energy inducing a therapeutic effect in biological tissue (Horvath, 1944) by mechanisms that are now

divided generally into thermal (Barnett and Kossoff, 1992) and non-thermal/mechanical effects (Barnett et al., 1994, 1997; Goss et al., 1978).

When tissue temperature is elevated (especially when induced artificially), the condition is called hyperthermia. Ultrasound is able to induce hyperthermia because the longitudinal propagating sound waves cause any particles in their path to begin to oscillate. These oscillations cause density changes in the medium thru which the sound is traveling. The medium resists the density change and energy is absorbed into the medium in the form of heat. In addition to thermal energy absorption, ultrasound can also be delivered in such a way that imploding gas bubbles create microjets of incredibly high pressure.

Ultrasound beams are usually generated using piezoelectric plates, generally made of certain types of crystals or ceramics. These materials deform mechanically in proportion to an applied electrical signal. The deformation of the material causes its surrounding medium (generally water or air) to deform as well. To produce ultrasound, the electrical signal sent to the piezoelectric plate must be an oscillating signal at a frequency exceeding 18 kHz.

Focusing of the ultrasonic longitudinal waves can be achieved using a spherically curved piezoceramic plate, with lenses, or by dividing a plate into uncoupled electronic pieces and adjusting the phase of the electric input signal sent to each piece to create the focus at the desired depth and location. With either method, ultrasonic waves enter the body at separate points and constructively interfere to create an intense pressure wave at the focus, the size

of which is determined by ½ the wavelength of the pressure wave. For example, at 1.5 MHz the focus will be 1 mm across. Elsewhere the pressure wave will interact destructively and attenuate the pressure wave. As the medium in which the ultrasound wave is moving changes, there is reflection of the wave as predicted by Snell's law, the extent of which depends on the velocity and incident angle of the ultrasound wave. For this reason, focusing ultrasound through homogenous tissue will allow a much smaller focal region than tissue with more heterogeneity. If the composition of the material is well known, a piezoceramic plate with uncoupled electronic pieces can be programmed to correct the aberrations induced by tissue heterogeneities (Clement et al., 2000; Hynynen et al., 2004, 2006; Thomas et al., 1996).

Much of the work with focused ultrasound has been done with an eye towards focused ultrasonic surgery (FUS). FUS uses focused ultrasound to heat tissue to the point of death and is currently being tested in clinical trials for ablation of uterine fibroids (Hindley et al., 2004; Tempany et al., 2003), breast tumors (Gianfelice et al., 2003; Zippel and Papa, 2005), liver and kidney tumors (Illing et al., 2005), prostate cancer (Ripert et al., 2010), and the treatment of essential tremor (Elias et al., 2013). Ultrasound used in this way has thus been very well characterized and controlled, including models that are able to predict lesion sizes and shapes (Hill et al., 1994; Hynynen et al., 1995; Lizzi and Ostromogilsky, 1987). Much of the work is based on what is known as the thermal dose model (Sapareto and Dewey, 1984).

1.7 Thermal Dose

Thermal dose is a mathematical model that relates the biologic effect in a specific cell type or tissue expected after a hyperthermia treatment of any (or varying) temperature and duration to the duration of a treatment at a given reference temperature, generally 43°C.

The thermal dose model suggested by Sapareto and Dewey (Sapareto and Dewey, 1984) and in common use today is based on the Arrhenius equation, first proposed by Jacobus Henricus van 't Hoff in 1884 and later expanded upon by Svante Arrhenius (Arrhenius, 1889). The Arrhenius equation is an empirical formula describing the temperature dependence of chemical reaction rates and is responsible for the general rule of thumb derived from the Arrhenius equation is for every 10°C increase in temperature, the reaction rate doubles. This model was quickly applied to protein denaturation in vitro, the results of which were compiled by Eyring and Stearn (Eyring and Stearn, 1939). As described by Dewey, the logarithm of the inactivation rate of the protein in question was plotted against the inverse of absolute temperature. If the same mechanism was causing the inactivation/denaturation, the plot should be a straight line. Activation energy can be determined from the slope of that line. This "straight line" Arrhenius relationship is also observable in mammalian cells from 43.5 to 57°C. As mammalian cells exhibit varying heat sensitivities, plots of different cell types have lines that are parallel but shifted (Dewey, 2009).

Henriques and Moretz then introduced the concept of using Arrhenius plots (derived from the Arrhenius equation) to describe temperature and exposure time dependence on irreversible tissue damage (Henriques and Moritz, 1947). They examined the extent of burns in pig skin after flowing water of varying temperatures over the skin for varying amounts of time.

Sapareto and Dewey's thermal dose model compared the biologic effect of any given hyperthermia treatment to the amount of time that same cell type or tissue would require for the same biologic effect at 43 °C, often written as equivalent-minute dose (t_{43}), cumulative equivalent minutes (CEM) or thermal isoeffect dose (TID). The model predicts that the biologic effect on tissues held at 45°C for 15 minutes will be the same as tissues held at 43°C for 60 minutes. The equation is as follows:

$$t_{43} = \int_0^t R\hat{}(T(\tau) - 43)\, d\tau$$

where $T(\tau)$ is the function of temperature over time in Celsius and R is simplified to 2 for temperatures greater than or equal to 43°C and 4 for temperatures lower than 43°C. The simplification of R, which is a function of activation energy and absolute temperature, causes an error of only 2% for temperatures ranging from 37 to 46 °C. At a constant temperature the equation reduces to

$$t_{43} = R\hat{}(T-43) * t,$$

meaning that for temperatures above 42°C every 1°C increase in temperature cuts the duration for the same biologic effect in half.

Often a threshold of t43 = 240 minutes is used as a conservative estimate of cell death (Damianou and Hynynen, 1994), due to protein denaturation and coagulative necrosis, although heat-induced cell death can and does occur at lower thermal dose values and through different mechanisms, and the exact threshold varies with tissue type (Dewhirst et al., 2003).

1.8 MRI Temperature Monitoring

Ultrasonic hyperthermia can be carefully monitored with several types of thermometry techniques, most notably MRI (Magnetic Resonance Imaging) because of its noninvasive nature. MRI provides excellent soft tissue contrast for diseased tissue segmentation, while temperature sensitive pulse sequences can be used to measure relative temperature changes (Chung et al., 1996; Ishihara et al., 1995; Samulski et al., 1992). Several studies have shown the feasibility of MRI-guided ultrasound surgery in vivo (Cline et al., 1995; Hynynen et al., 1996; McDannold et al., 1998; Stepanow B et al., 1995), and shown that MRI thermal dosimetry techniques can be used to accurately predict the extent of thermal tissue damage (Chung et al., 1999; Hazle et al., 2002). MRI-guided focused ultrasound has been FDA approved for the ablation of uterine fibroids and for palliation of bone metastases.

MRI works by applying a strong magnetic field to a body, causing any atoms that have a magnetic moment due to a nucleus with non-zero quantum mechanical spin (the sum of the spin of the unpaired electrons) to line up with the magnetic field. Note that these atoms can line up in two directions, either aligned with the field or counter-aligned. If the atoms were split evenly between the two directions, there would be no net magnetization from the atoms because they would cancel each other out. Atoms aligned with the magnetic field have nuclei in a slightly lower energy state, and thus a small majority of the atoms lie in that direction. This causes a net magnetization in the same direction as the applied magnetic field. The protons in the atoms continue to wobble like a toy top along this magnetic field however, and the rate of the wobble is called the resonance frequency. This frequency is directly proportional to the strength of the magnetic field. In humans, the largest populations of atoms with non-zero spin are those of hydrogen in the water that composes two thirds of the body. If an RF pulse at the resonance frequency is applied, the atoms are excited to the higher energy state, causing them to flip their spin. This process causes the net magnetization vector to move out of plane as it travels the 180° needed to flip. When the RF pulse is turned off, the atoms return to the lower energy state alignment and release a photon with a frequency at the resonant frequency. These photons are then detected with an RF coil. The time it takes for longitudinal magnetization to return to its base state is called T1 relaxation, because it occurs exponentially with a time constant then named T1. The loss of phase coherence in the transverse plane is called T2 relaxation for the same reason. These times vary among tissues, and by manipulating the timing of the excitations and readouts, one can create different contrast between tissue structures. To make images, the magnetic field is

manipulated with special electromagnets called gradient coils. Since the resonant frequency is proportional to the strength of the magnetic field, one can manipulate which spins are excited (to select a slice or volume) and create a situation where the frequency and phase of the RF emissions that occur during relaxation vary spatially (Hashemi et al., 2010).

MRI temperature monitoring works by utilizing the changes in hydrogen bonds that occur with changes in temperature in water (Hindman, 1966; Ishihara et al., 1995; De Poorter et al., 1995). As water is heated, the hydrogen bonds bend and break, resulting in an increase on average in electron shielding of the hydrogen nucleus. This increase shielding reduces magnetic field at the nucleus. Since the resonant frequency is proportional to magnetic field, a temperature increase thereby reduces the proton resonance frequency. This change in resonant frequency, which changes with temperature at approximately -0.01 ppm/°C (Hindman, 1966), can be readily measured by recording the phase of the MRI signal in addition to the normally acquired magnitude (Ishihara et al., 1995). The frequency can be estimated by dividing the phase by 2□ times the duration in which the phase was allowed to develop. While the temperature dependence is small, it is possible to create temperature maps with noise levels less than ±1°C. Since the magnetic field is not perfectly homogeneous, only *relative* temperature measurements can be made with MRI by subtracting a phase map obtained before the heating began. The need to use image subtraction makes the method sensitive to motion. Another limitation of the method is its insensitivity to temperature changes in lipids, which do not have hydrogen bonds.

1.9 Heat Shock Proteins

It has been suggested that heat shock proteins (HSP) promoters could be used to spatially and temporally control gene therapy delivery. HSPs, also called stress proteins, are a group of proteins discovered in 1962 (Ritossa, 1962) that are expressed when a cell undergoes various types of environmental stresses such as heat, cold and oxygen deprivation. There are five families of HSPs categorized generally by molecular weight; Hsp90, Hsp70, Hsp60, Hsp10, Hsp100 and the "small HSPs (sHsp)". HSPs are a highly conserved protein and are universally present in almost all eukaryotic cells from bacteria to human (Gupta and Singh, 1994; Hunt and Morimoto, 1985; Lindquist and Craig, 1988). Since *HSP* genes are so highly conserved, *HSP* promoters can be used trans-species. HSPs also show the most selective and inducible transcription regulation in any eukaryotic cell (Kregel, 2002; Voellmy, 1994). Hsp70 is the one of the most strongly induced of the family and the quickest to be repressed again after the stress event (DiDomenico et al., 1982). The mechanisms involved in the activation of HSP gene promoters are not yet completely understood. It is known that the *Hsp70* promoter has multiple adjacent and inverted iterations of the pentanucleotide motif 50-nGAAn-30, which are called heat shock elements (HSE) (Fernandes et al., 1994). These HSEs interact with heat shock factor 1 (HSF1) to activate transcription. HSF1 is normally bound to Hsp90. Heat breaks down that bond and HSF1 forms homotrimers which then translocate to the nucleus to bind to HSEs on the promoter. RNA polymerase II is normally trapped in the open reading frame of a TATA element on the *Hsp70* promoter, causing what is known as post-transcriptional pausing. HSF1 trimers bind to the HSE of

the promoter, releasing the pause and allowing transcription to continue (Tang et al., 2000).

Hsp70 is a general name for what is actually a family of 12 proteins in humans, some of which are stress-inducible and some are not. The *Hsp70b* gene is located on chromosome 1 and has been renamed *Hspa7* by the HUGO Gene Nomenclature Committee, although it is still referred to as *Hsp70b* in the majority of scientific literature.

The *Hsp70b* promoter is the most potentially useful heat-activated promoter as it has been shown to be activated only by the stress of heating and there are magnitudes of difference between induced protein expression versus the basal expression (Hildebrandt et al., 2002). Protein expression for 24 hours after a heat shock is comparable to that induced by using the Cytomegalovirus (CMV) vector (Gerner, et al. 2000; Borrelli, et al., 2001). Modifications to the *Hsp70b* promoter have been shown to induce even higher expression (Borrelli et al., 2001; Brade et al., 2000; Gerner et al., 2000).

1.10 Previous Work using HSP-Promoted Gene Therapy

Previous work using *HSP* promoter gene therapy constructs has shown that *in vitro* gene expression increased linearly with heating duration after reaching a threshold temperature (Smith et al., 2002) . Borrelli et al. also demonstrated significant induction *in vitro* after exposure to temperatures greater than 40°C. The magnitude of the induction increased

from 41 to 43°C and varied with the duration of heating (Borrelli, et al 2001). Others obtained similar results *in vitro* using temperatures up to 48°C with reduced exposure times of 30 to 180 seconds (Brade, et al., 2003; Gerner, et al. 2000; Vekris, et al. 2000).

Hsp70b-promoted gene therapy has been used *in vivo* to spatially control expression of cytotoxic transgenes, reducing tumor size in animal models of melanoma, breast cancer, and glioma (Braiden, et al., 2000; Huang, et al., 2000; Lohr, et al., 2000; Vekris, et al., 2000). Smith et al. have shown the utility of this system for targeted induction using an adenovirus containing the cytotoxic Fas ligand gene under the control of the *Hsp70b* promoter (Smith, et al., 2002). That study showed the systemic delivery of the Fas ligand adenoviral construct did not lead to liver toxicity unless the animals were exposed to ultrasound-mediated hyperthermia. Other experiments making use of this ultrasonic heating methodology were able to show heat-induced gene expression in rats after a 3 minute exposure to temperatures from 40-50°C, as well as in mice after a 25 minute exposure at 43°C (Guilhon, et al., 2003).

Investigations into how expression of *HSP*-promoted proteins changes with different temperatures and durations of heat shock are more limited. O'Connell-Rodwell found that there are actually 5 "levels" of hsp-promoted gene expression using a murine *Hsp70A* promoter with the luciferase reporter gene (O'Connell-Rodwell, et al., 2004). At low temperatures (<42°C) no matter what the duration, no gene expression was found (level 1). At slightly higher temperatures (e.g. 43°C) for 20 minutes, reporter activity was

present and peaked around 4 hours post heat shock (level 2). However, after heating cells to 45°C for the same amount of time, the peak reporter activity level was found at 6 to 8 hours after heat shock (level 3). Level 4 is defined as much higher temperatures for short durations (e.g 50°C for less than 15s). At this level, the reporter gene activity is quite low, but the cells themselves are found to be viable. Despite the low concentrations of reporter proteins, large quantities of the reporter gene mRNA were found in comparison to levels 1-3. ATP levels at this level were found to be low. Level 5 is defined as temperatures and durations that resulted in cell death.

In 2010, Rylander and et al. explored the relationship of hyperthermia protocols with HSP expression kinetics in order to develop corresponding computational predictive models of normal and cancerous prostate cell response (Rylander et al., 2010). As previously shown, they found that increasing heating durations at 44°C increased Hsp70 expression at 16 hours post-heating using Western blot analysis. Maximum Hsp70 expression in PC3 cells was found using a heating protocol of 50°C for 1 min, which expressed 2.7 times the control. Using research previously published calculating HSP expression via laser therapy heating by the same authors (Rylander et al., 2006), a model of the form

$$H(t,T) = Ae^{(\alpha(T)t-\beta(T)t^{\gamma(T)})}$$

was proposed as a computational model of Hsp70 production kinetics, where H(t,T) is the Hsp70 expression at 16 hours post-heating, T is the heating temperature and t is the

heating duration. $\alpha(T)$, $\beta(T)$, and $\gamma(T)$ are kinetic parameters are independent of time but dependent on temperature. Using non-linear least square regression, these kinetic parameters were calculated based on the experimental results discussed above. The resulting calculated values were compared to experimental results. Correlation coefficients were generally greater than 0.9 for different heat shock durations at the same temperature. However, the calculated kinetic parameters did not appear to follow any discernible pattern with α ranging from -7.7 to 174.15, β from -4.39 to 173.32, and γ from 1.01 to 10.6 as the heat shock temperature changed.

1.11 Activation of Hsp70 due to Mechanical Stress

The previous sections show successful attempts to test activation of *HSP*-promoted gene therapy with ultrasonic hyperthermia. However, as ultrasound causes both mechanical and hyperthermic stress, several papers have investigated whether mechanical stress alone can activate HSPs. In 1990, Angles et al. demonstrated that exposure to ultrasound without any temperature change did induce Hsp71/73 in rat embryos. Nussbaum and Locke found that Hsp72 can be induced with mechanical stress through ultrasound, reversing their previous conclusions (Locke and Nussbaum, 2001; Nussbaum and Locke, 2007).

However, studies looking at Hsp70 and Hsp70b specifically are less available. Xu et al. showed that Hsp70 proteins could be activated by mechanical stress caused by a Cyclical Stress Unit (Xu et al., 2000) but also mentioned that previous work had shown the

opposite (Sadoshima et al., 1992). Using Western blot analysis, they attributed the effect to HSF1 activation and suggested that the effect might be cell-type dependent.

A study by Hundt and al. looked at whether mechanical stress activated *Hsp70A.1* promoters in three different tumor cells lines (Hundt et al., 2007). Cells were suspended in solution in what they describe as "1.5 mL conical thin-walled thermocycler tubes (E & K Scientific, Campbell CA)" and heated in either a thermocycler or a 36°C waterbath. The samples heated by waterbath were monitored with thermocouples inside the tubes. Ultrasound was applied with two different methods, either intensity increased while the pulse duration remained constant or the intensity stayed constant while pulse duration increased. They found that the method of ultrasound application did not significantly affect expression levels. However, they did find that lower temperature heat shocks caused the sonicated cells to produce higher levels of gene expression at lower temperatures than the cells that were only heated. The effect reversed itself at higher temperatures.

Deckers and al. also explored the issue of whether the mechanical stress associated with ultrasonic heating activated the *Hsp70-1B* promotor (Deckers et al., 2009). NLF-1 transgenic mice were transfected with a luciferase gene under the control of the *Hsp70-1B* promoter and exposed to two ultrasonic protocols that delivered the same amount of acoustical energy (125J) at the same pressure amplitude. The first protocol heated the tissue but the second lowered the duty cycle of the ultrasound application to 20%,

producing only a negligible temperature increase. The results showed no luciferase expression in the tissue area exposed to the non-heating ultrasound protocol.

Lui et al. in 2005 explored mechanical stress activating Hsp70b in particular (Liu et al., 2005). Similarly to Hundt et al. study discussed above, a 10μL cell suspension in a thin-walled PCR tube was placed in line with the ultrasonic beam focus of a 1.1MHz ultrasound transducer. The duty cycle was changed to achieve different temperature elevations in the cell suspension while keeping the pulse repetition frequency constant. Temperature was measured by a bare-wire thermocouple. The cell suspension had a non-uniform spatial temperature fluctuation of up to 3°C. Passive cavitation was monitored by a 15MHz transducer. The cells that were to be heated but not sonicated were grown on a cover slip and plunged into a heated PBS solution for 2 seconds. All cells were lysed and processed for cell viability and gene expression quantification 24 hours after heating. Looking at heating temperatures of 50-70°C for short time bursts, they found that mechanical stress contributes to cell damage and thus to cell viability, but it does not elicit a measureable stress response. They continued this work in 2006, looking at *Hsp70b* gene activation in human tumor-implanted mice (Liu et al., 2006). Using a 3.3 MHz transducer to reduce cavitation, they compared tumors which had been subjected to hyperthermia via continuous ultrasound against tumors subjected to the same total acoustical power but with a much reduced duty cycle thus causing no significant heat increase. They found that the cells subjected to only mechanical stress exhibited a 4-fold increase in gene expression over the control, compared to the 170-fold increase in the cells subject to both hyperthermia and mechanical stress.

2 Feasibility of Spatial and Temporal Control of Gene Expression *in Vivo*

2.1 Motivation

In this study, ultrasound is examined for facilitation of gene therapy delivery in the context of spatially controlling therapeutic protein production. By attaching the gene of interest to an *Hsp70b* promoter before placing it in the viral vector construct the gene is prevented from being transcribed into RNA under normal conditions. The cell will produce minimal amounts of the therapeutic protein until the cell is heated to the point that the *Hsp70b* promoter drives transcription of the gene of interest. Ultrasound can be utilized to heat the gene under minimally invasively conditions after delivery into the cells. We were interested in the feasibility of inducing reporter protein production only in the ultrasonically-heated lobe of the canine prostate after injecting the *Hsp70b*-reporter gene construct to the entire prostate.

The work described in this chapter has been previously published in *Ultrasound in Medicine and Biology* (Silcox et al., 2005).

2.2 Materials and Methods

2.2.1 Development of gene vector

Recombinant adenoviral vectors were generated by standard techniques using the shuttle plasmid pACCMV-pLpA and pJM17 as described by Becker et al. (1994), which uses recombination in 293 cells to generate a replication-defective serotype 5 adenovirus. In these constructs, an expression cassette containing a minimal human *Hsp70b* promoter and RNA leader sequences upstream of the transgene with a 3'rabbit β-globin splice site

and poly-adenylation sequences replacing the CMV promoter and SV40 polyadenylation signal sequences from pACCMV-pLpA, as described previously by Smith et al. (2002). The viral construct (Ad-HSP-Luc) contains the transgene, firefly luciferase, under transcriptional control of the *Hsp70b* promoter.

2.2.2 Gene transfer into prostate

All animals were cared for in accordance with Brigham and Women's Hospital's animal care policy. Three beagles ranging in size from 13-17 kg were anesthetized using a mixture of 200mg of ketamine hydrochloride (Abbott Laboratories, North Chicago, IL) and 20 mg of sodium xylazine (Xyla-ject, Phoenix Pharmaceuticals, St. Joseph, MO) injected intramuscularly. Using a transrectal ultrasound imager, the prostate was visualized and catheters were inserted either just below the rectum or through the abdomen and into each lobe of the prostate. The purified virus was then injected into each lobe of the prostate (1 ml of solution in each lobe, consisting of 1×10^9 pfu in saline), followed by a saline wash. The animals were then allowed to wake naturally and pain was controlled using twice-daily 0.07 mL/kg intramuscular injections of buprenorphine hydrochloride (Buprenex, Reckitt Benckiser Pharmaceuticals Inc., Richmond, VA).

2.2.3 Heat Induction

48 hours after the virus injection, the animals were again anesthetized with the same mixture of ketamine and xylamine; then intubated. Hydration was maintained with a saline IV drip. The procedure was monitored with a 1.5 T clinical MRI unit (GE Medical Systems, Milwaukee, WI). The ultrasound field was created using an unfocused, 1.5 MHz, air-backed transrectal transducer (Smith et al. 1999).

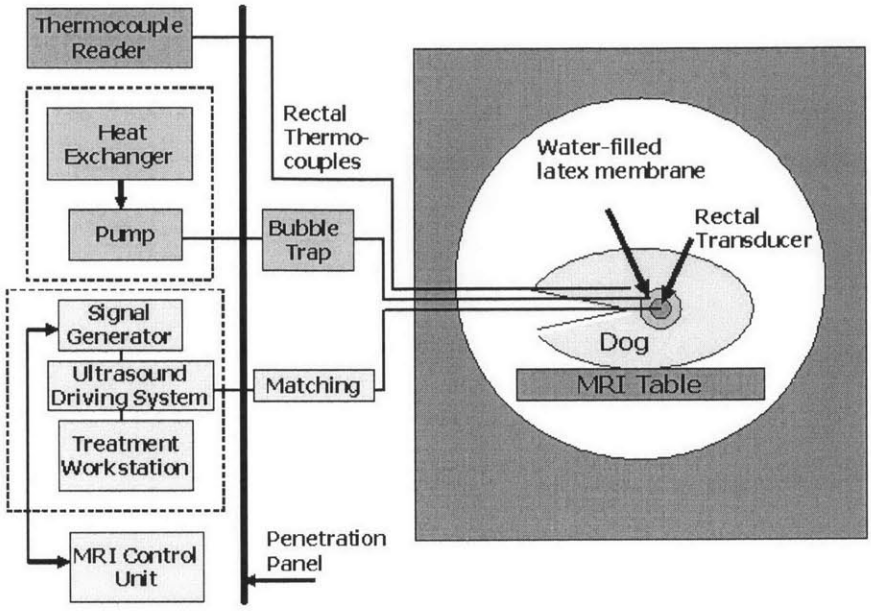

Figure 2-1: Experimental set-up for heat induction.
A transrectal ultrasound transducer surrounded by a water-filled latex membrane was placed in the rectum of the animal. The sonication was driven by an RF system while MRI and thermocouples monitored temperature

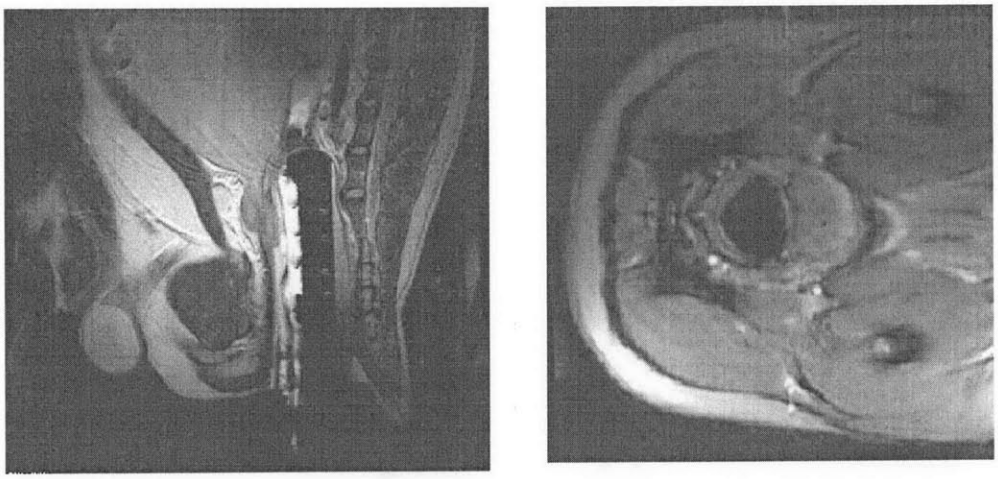

Figure 2-2: MR images of the transducer inserted into the rectum and positioned next to the prostate. A latex membrane surrounding the transducer is expanded using heated degassed water and covered with ultrasound gel to remove air pockets between the transducer and rectum. (a) Coronal image (fast spin echo T2 weighted image TR/TE 2000/75ms, echo train length 8, field of view 24 cm, number of excitations 2) (b) Axial image (the magnitude of fast spoiled gradient-echo imaging described in text).

The transducer was made of four 120 degree sections of cylindrical PZT-8 material (lead zirconate–titanate, EC-69, EDO, Salt Lake City, UT) with a length of 15 mm. Each of these pieces were placed along the primary axis of the transducer shaft and scored on the inner electrode surface. This divided each piece of PZT into four individually powered and controllable sections, creating a total of 16 independent channels. A multi-channel RF driving system, constructed in-house (Daum et al., 1998), was used to control power delivery.

The prostate was found through palpitation and MR imaging and thermocouples were inserted into each lobe. MR imaging confirmed the correct positioning (Figure 2-2). The transducer was then inserted into the rectum and the latex membrane (Civco, Kalona, IA) surrounding the transducer was then inflated to fit snugly against the rectal wall using degassed water continually circulated at body temperature using a heat exchanger and pump. Ultrasound coupling gel (Aquasonic 100; Parker, Orange, NJ) was used to eliminate air pockets between the latex membrane and rectal wall. A heating pad was placed around the animal to maintain its body temperature.

Temperature was monitored using both MR thermometry and four copper-constantan thermocouples placed in each lobe of the prostate, between the rectal wall and the heated balloon, and externally. The thermocouples were constructed in house of 50 μm diameter copper and constantan wire (California Fine Wire Co., Grover Beach, CA) connected by soldering. The wires were incased in a fused silica sleeve used to guide the thermocouple

through a catheter to the prostate. The bare junction extended outside of the tubing approximately 5 mm to minimize viscous heating artifacts (Fry et al., 1954; Hynynen and Edwards, 1989). As the temperature changes at the solder joint, a voltage is generated that can be measured and converted to temperature by a commercially available thermocouple reader (TC1000, Sable Systems, Henderson, NV).

MR thermometry was performed as described elsewhere (Smith et al. 1999). Briefly, temperatures were measured by exploiting the temperature dependence of the proton-resonant frequency (Ishihara et al. 1995). Changes in the proton-resonant frequency were estimated by measuring changes in phase and dividing by 2π times the time in which the phase developed (the echo time of the image). A fast spoiled gradient-echo sequence was used to acquire the phase maps (Chung et al. 1996). The following parameters were used: 39.5ms/19.3ms (repetition time/echo time); flip angle, 30°; bandwidth, 3.57 kHz; field of view, 20 cm; section thickness, 5 mm; matrix size, 256 x 128; imaging time, 5.2 seconds. The temperature dependence of the proton-resonant frequency shift was assumed to be 0.010 ppm/°C, the value used by Chen *et al.* (2000) when monitoring experiments in the human prostate. A set of four axial images were taken approximately every 40 seconds to average out noise, then imaging was paused to allow a thermocouple measurement without MR interference, and then the next set of four images were acquired.

By using only the ultrasound channels that lined up with the left lobe of the prostate, we were able to limit the hyperthermia exposure to that area in 2 of the 3 dogs. RF powers up

to 70 W were used to heat and maintain the sonicated area at the desired temperature. The procedure continued until the temperature of the left lobe was at or above 42°C for 25 minutes, as measured by the thermocouple.

2.2.4 Sacrifice

Animals were sacrificed 15-20 hours after the heating using a 0.13 ml/kg intravenous injection of Euthasol (Delmarva Laboratories, Midlothian, VA, USA). The prostate was removed, sectioned and flash-frozen using liquid nitrogen and stored at -80°C for processing.

2.2.5 Analysis

The prostate was sectioned by four axial cuts into five pieces, labeled 1-5 from most superior to most inferior. Sections 1, 3 and 5 were ground with a mortar and pestle under liquid nitrogen. The resulting powder was dissolved in Promega reporter lysis buffer (Promega Corporation, Madison, WI) containing protease inhibitors and assayed (2 μl) using the Promega luciferase assay reagent (100 μl). Light measurements were made with a luminometer (Berthold Lumat LB9501, Nashua, NH) over 10 seconds and measured as light units per microgram of protein. Protein was measured using the bicinchoninic acid (BCA) method first described by Smith *et al.* (1985) (Pierce Chemical Co, Rockford, IL) with BSA as a standard.

Thermal dose was calculated from temperatures from the middle of each lobe in dogs 1 and 2 using the equation set forth by Sapareto and Dewey (Sapareto and Dewey 1984). This equation is used to equate the range of actual temperatures during the experiment with an "equivalent" time at a reference temperature of 43°C that would have the same cellular response.

2.3 Results

The temperature progressions during the experiments in the left (treated) and right (untreated) lobes of the animals' prostates are shown in Figure 2-3 alongside the electrical power delivered. The temperature data from dogs 1 and 3 was extracted from the thermocouples placed in the left and right lobes of the prostate during the experiment. With the first dog, a temperature difference was maintained throughout the experiment, with the left lobe measuring 42°C or greater for 29 minutes and the right lobe measuring less than 42°C throughout the experiment. Note that power was continually increased to compensate for temperature decreases, likely due to increased blood flow resulting from the homeostatic vasodilation response to heat. In Dog 3, because of the small size of the prostate, it was not possible to limit heating to only one lobe with the experimental set-up used. Thus, the left and right lobe temperature measurements were equal to or greater than 42°C for 24 and 23 minutes, respectively, during 35 minutes of heating.

In dog 2, the left thermocouple was dislodged mid-experiment, which necessitated the use of the MR thermometry data to review the temperature progression during the 104

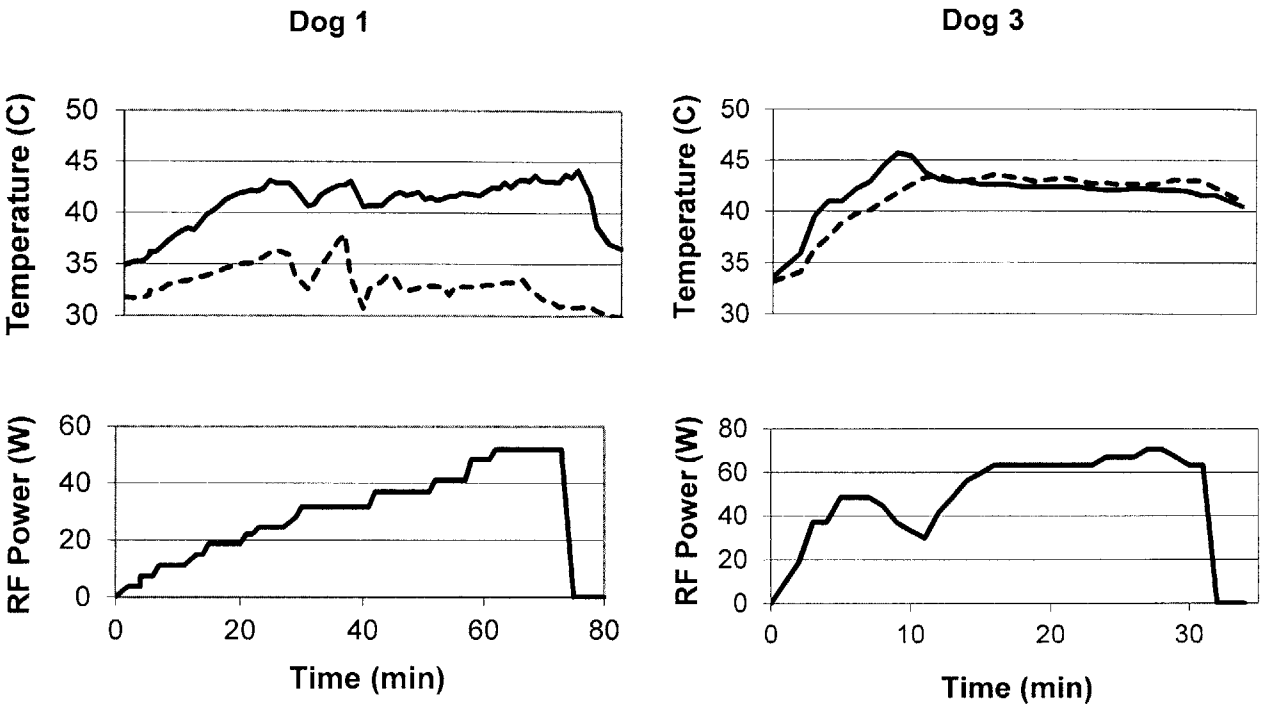

Figure 2-3: Temperature maps of the prostate lobes during heat induction in dog 1 and dog 3. The left lobe temperatures are marked with a solid black line and the right lobe temperatures are marked with a dashed black line. Temperature data is from thermocouples placed in the middle of each lobe. The lower graph shows the RF power delivered to the transducer at each point during the experiment.

minute long experiment. The majority of heating occurred between 12 and 20 minutes, between 75 and 85 minutes and between 90 and 97 minutes into the experiment. Figure 2-4 shows the temperature delineation of the left and right lobes during the heating, as measured by MRI, in dog 2. Signal intensity increases with temperature and the lower temperature in the right lobe of the prostate is clearly distinguished from the higher temperature in the left lobe at 12 minutes and 79 minutes into the experiment.

Thermal dose was calculated using temperatures from the middle of each lobe using thermocouple data in dogs 1 and 3 and MR thermometry in dog 2. Dog 1 had a thermal dose of 29.7 minutes in the left lobe and less than 0.01 minutes in the right lobe while

dog 2 had a thermal dose of 71.9 minutes in the left lobe versus 3.7 minutes in the right lobe. The third dog received 27.1 equivalent heating minutes in the left lobe and 22.3 minutes in the right.

The luciferase activity observed in each lobe of the prostate for the three animals is shown in Figure 2-5. Dog 1 shows a 31-fold increase in activity in the left (treated) versus the right (untreated) lobe, while dog 2 shows a 14-fold increase and dog 3 shows no significant difference in luciferase activity between the two lobes.

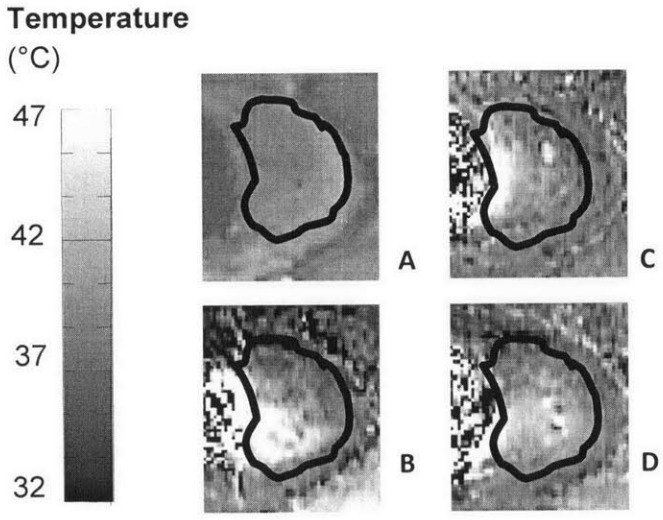

Figure 2-4: MRI temperature maps of Dog 2.
(a) An MRI image (the magnitude of fast spoiled gradient-echo imaging described in text) of Dog 2 before heat induction with the prostate outlined in black. The next three images are temperature maps (MR parameters described in text) of the same area at **(b)** 12, **(c)** 39 and **(d)** 79 minutes into the experiment. Note that signal intensity increases with temperature and that the lower temperature of the upper (right) lobe of the prostate is clearly delineated from the higher temperature of the bottom (left) lobe in (a) and (c).

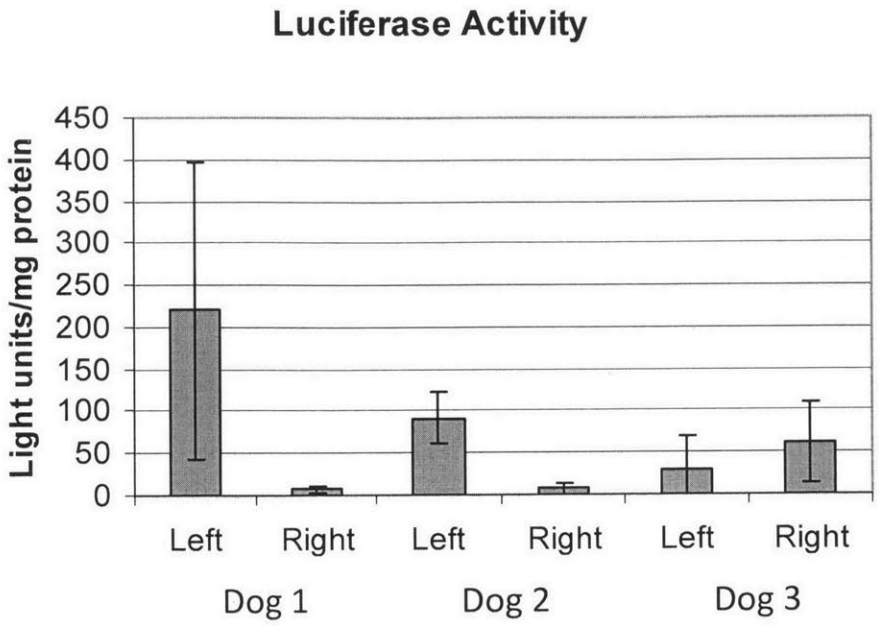

Figure 2-5: Luciferase activity in the three animals, separated into each lobe. Dog 1 shows a 31-fold increase in activity from the left to the right lobe, while dog 2 shows a 14-fold increase and dog 3 shows none.

2.4 Discussion

We have successfully used MRI-guided, ultrasound-induced hyperthermia to spatially control gene expression in an animal model relatively close to human in size. The luciferase expression in dogs one and two was 31 and 14-fold higher, respectively, in the heated lobe versus the control lobe. Dog three, in which both lobes were heated, showed no significant difference in luciferase expression between the lobes.

The temperatures in these experiments were monitored in two ways, by MRI thermometry and by thermocouples inserted into the animal. In the clinic, MR would be the preferred temperature monitoring method due to its non-invasive nature and for its ability to allow continuous monitoring in multiple planes, allowing any unwanted heating

to be identified and corrected. There are limitations when using MR thermometry (as reviewed by Quesson (Quesson et al., 2000) since temperature measurement is based on the changes in phase relative to an image acquired before heating, any movement by the subject disrupts the alignment between the images and the continuity of the temperature measurements is lost. Fortunately in a clinical situation both the situations could be controlled either by pausing the experiment to regain temperature integrity or by using MRI thermometry sequences less sensitive to motion (Kuroda, 2005). It is also possible to use surrounding unheated tissues to create a simulated baseline image (Rieke et al., 2007). In addition, blood flow in large vessels could also cause artifacts in the MRI-derived temperature maps.

Smith et al (2002) showed that gene expression increased linearly with the duration of heating. In this work, dog 1 received the longest duration of heating above 42°C and the highest level of luciferase activity was observed in the left lobe of this animal. In contrast, both lobes of the dog 3 prostate and the left lobe of the dog 2 prostate were heated above the 42°C threshold temperature for 4-5 minutes less and all had a comparably lower level of luciferase activity than the left lobe of dog 1. Madio *et al* (1998) examined intrinsic heat shock protein expression *in vivo* with MR-monitored ultrasonic heating of the rat leg to temperatures ranging from 42-45°C for forty-five minutes. They found that Hsp70 expression increased from 3 to 67 fold compared to unheated muscle tissue. This agrees well with the 14 and 31 fold induction of luciferase expression reported in this study, despite the difference in tissue type.

A point of considerable interest was whether the induction of the *Hsp70b* promoter was simply the result of reaching a threshold temperature or if the level of expression was related to a more complicated relationship between heating duration and temperature, as has been found in hyperthermia experiments measuring the extant of necrosis. Comparable levels of induction have been obtained in vitro by Borrelli *et al.* (2001) and Vekris *et al.* (2000) at temperatures ranging from 41°C for 4 hours to 48°C for 30 seconds, conditions which resulted in thermal doses that are approximately equal. The small number of animals in the current experiment did not allow any conclusions to be drawn regarding this question, partially due to the pattern of heating in dog 2. In that animal, the thirty minute long heat treatment was performed in two phases with significant cooling between the phases. This discontinuity of heating may be important since it has been shown *in vitro* that cells develop thermotolerance after exposure to non-lethal heating that can inhibit heat shock protein induction after a second heat treatment (Li and Mak, 1989; Mizzen and Welch, 1988). During ultrasonic heating, animals are periodically able to regain temperature homeostasis through vasodilation, which increases blood circulation to the heated tissue to cool the area (Lehmann and De Lateur, 1990). When the power is increased to return to the hyperthermic temperature range, periods of heating are interspersed between intervals at lower temperatures. Although the time intervals are much shorter than those generally used when investigating thermotolerance, the inability to correlate reporter expression with thermal dose in this study suggests the possibility of thermotolerance or a more complex relationship. Further studies are needed to determine how the temperature and duration of treatment might affect the extent of transgene expression from the *Hsp70b* promoter.

This preliminary study supported the concept that transgene constructs under control of the *Hsp70b* promoter could be used in conjunction with MRI-guided ultrasound heating to spatially control gene expression. The unfocused 16-element array used in this study allowed only limited control of the field being heated. It would be useful in the future is to utilize a focused transducer to determine the extent of spatial resolution that can be achieved with ultrasound mediated control of gene expression. More sophisticated phased array applicators could provide greater control of temperature and volume (Hutchinson and Hynynen, 1998), which would enhance the utility of this method. The next step would be to vary thermal conditions and the duration of treatment to determine if the amount of protein expression using this method of control were to be possible to predict.

3 Evaluating the Predictability of Hsp70b Activation Kinetics

3.1 Motivation

In the previous study, a detailed relationship between heating temperature and duration and protein expression was not quantifiable. Here, a step back was taken to examine these parameters in more detail using *in vitro* cell cultures. The first purpose of this section was to determine the repeatability of *Hsp70b* mRNA production kinetics at a specific heating profile (heat shock duration and temperature). In addition, the amount of *Hsp70b* mRNA produced during varying heating profiles was to be examined to determine patterns or relationships, such as thermal dose. mRNA expression, as an early measurable quantity of gene transcription, was used as the parameter for gene activation. This was chosen to eliminate as many other cellular factors as possible that might affect the result.

3.2 Materials and Methods

3.2.1 Cell Growth

HeLa cells, a commonly used human ovarian cancer cell line, were grown on 15 cm tissue culture plates. Growth media was made with 500mL Cellgro DMEM media (Corning Inc.; Corning, NY) containing 2.75mg glutamine (Corning Inc.) supplemented with 50mL fetal bovine serum (BioWhitaker, Lonza; Basel Switzerland), 50,000 units of penicillin (Gibco, Life Technologies; Grand Island, NY) and 50mg of streptococcus (Gibco). The cells were incubated in a Revco Ultima 37°C humidified chamber (Thermo Scientific; Tewksbury MA) set at 5% CO_2. Cells were harvested for experiments at 90% confluence.

3.2.2 *Waterbath Experiment Heating Protocol*

Seven experimental conditions were tested in triplicate; heating for 15 minutes, 30 minutes and an hour at 43°C, and heating for 15 and 30 minutes at 44°C and 45°C. The cells were heated to the specified experimental temperature using a Precision circulating waterbath (Jouan Inc., Winchester VA). After the water was heated, a sterilized thermocouple was attached to a 50mL centrifuge tube with 40mL of HeLa growth media. The tube was placed in the waterbath to heat to the desired experimental temperature, which took approximately 30 minutes.

Meanwhile, the plated HeLa cells were detached from the plates using 2mL of .25% Trypsin-EDTA (Gibco) per plate and quantified using a Bright-Line hemacytometer (Haussel Scientific; Horsham, PA). 1.6 $x10^{-6}$ cells per timepoint were placed in a 10mL centrifuge tube. A final sample of 1.6 $x10^{-6}$ cells was placed in a separate tube to use as an unheated control. Both tubes were capped loosely and placed back in the incubator for 30 minutes to recover.

The cells were removed from the incubator and centrifuged to a pellet at 1000 rpm for 5 minutes. The pellet was re-suspended in 1mL of room temperature growth media, which was then added to the 50mL centrifuge tubes filled with warmed media in the water bath. The introduction of the cells temporarily reduced the temperature of the warmed media by 0.2 to 0.5°C. For experimental timepoints that occurred during the heating process, the cell suspension was mixed with a pipet before removing 7mL of the suspension, causing

another small temperature decrease. When the experimental heating time was concluded, the cell suspension was removed from the water bath and left at room temperature until temperature of the media decreased below 42°C, which occurred within 60 seconds.

3.2.3 Post-Heating Protocol

The cell suspension was centrifuged at 1000 rpm for 5 minutes and the medium replaced before dividing the suspension into separate 10mL centrifuge tubes, one for each timepoint sample. The tubes were loosely capped and placed in the 37°C incubator.

Samples were taken at least five timepoints: 0 minutes (a non-heated control), 15 minutes after the start of heating, 30 minutes, 1 hour, 2 hours, and 4 hours. Some experiments required additional timepoints from 6 to 24 hours to fully characterize the mRNA kinetics. At each timepoint the cells were removed from the incubator and lysed according to the standard procedure described in the RNeasy Mini Kit (Qiagen; Venlo, Limburg) using a QIAshredder. The suspension was mixed with 350 µg RNase-free 70% ethanol (Sigma-Aldrich; St. Louis, MO) and stored at -20°C until the RNA could be isolated.

3.2.4 Analysis

RNA was isolated from each sample using the standard procedure in the RNeasy Mini Kit with the optional DNase removal step using the RNase-Free DNase Set (Qiagen). The RNA was quantified and checked for purity using a SmartSpec Plus spectrometer (Bio-Rad; Waltham, MA), and 2 µg of RNA was used to make cDNA using a High Capacity

cDNA Reverse Transcription kit (Applied Biosystems; Grand Island, NY) and a 7300 Real Time PCR System (Applied Biosystems).

The relative amount of hsp70B in each cDNA sample was quantified using RT-PCR with β-actin acting as the control. The primers were designed using Primer-Blast, the primer design tool on the National Center for Biotechnology Information's (NCBI) website, and ordered from Integrated DNA Technologies (Coralville, IA). The primer composition was as follows:

Hsp70b forward primer	5'- ACC TTC CCC GCA TTT CTT TCA GCA - 3'
Hsp70b reverse primer	5'- CCG CGG TAG CAT ACG CGC A - 3'
β-actin forward primer	5' – AAA AGC CAC ACT TCT CT - 3'
β-actin reverse primer	5' – CTC AAG TTG GGG GAC AAA AA - 3'

FastStart Universal SYBR Green Master Mix (Roche; Basal, Switzerland) was used for the florescence dye, nucleotides and Taq DNA polymerase needed for the RT-PCR reaction. A disassociation curve was produced during each RT-PCR test to check for dimers. Each experimental time series was tested in triplicate on individual plates.

3.3 Results

Temperature was monitored during all waterbath experiments with a TC-1000 Thermometer (Sable Systems International; Henderson, NV). Figure 3-1 shows typical examples of heating at 43°C for 15, 30 and 60 minutes. There was a brief decrease in temperature of about 0.25°C when the cells were inserted. In the 30 and 60 minutes experiments, there were similar dips at the 15 and 30 minute timepoints, as cells were removed for lysing. Temperatures during the experiments were within ±0.5°C of the target temperature throughout the duration of the cell heating, although the average temperature was generally slightly below the target temperature.

After isolation of the RNA samples at each timepoint, the concentration and purity of the RNA was tested with SmartSpec Plus spectrometer (Bio-Rad; Waltham, MA). Concentrations ranged from 242 to 814 μg/mL, averaging 458 μg/mL. Purity was defined by its A260/A280 rating and ranged from 1.5 to 1.8, which are acceptable levels.

To determine the relative concentration of *Hsp70b* mRNA produced, the isolated RNA was converted to cDNA and rt-PCR was performed, measuring both β-actin and *Hsp70b* cDNA levels. C_T numbers were calculated with a common threshold level of 0.8.

To normalize the amount of cDNA in each sample, the C_T of β-actin was subtracted from the C_T of *Hsp70b*. This allows the cDNA to be directly related to the amount of mRNA

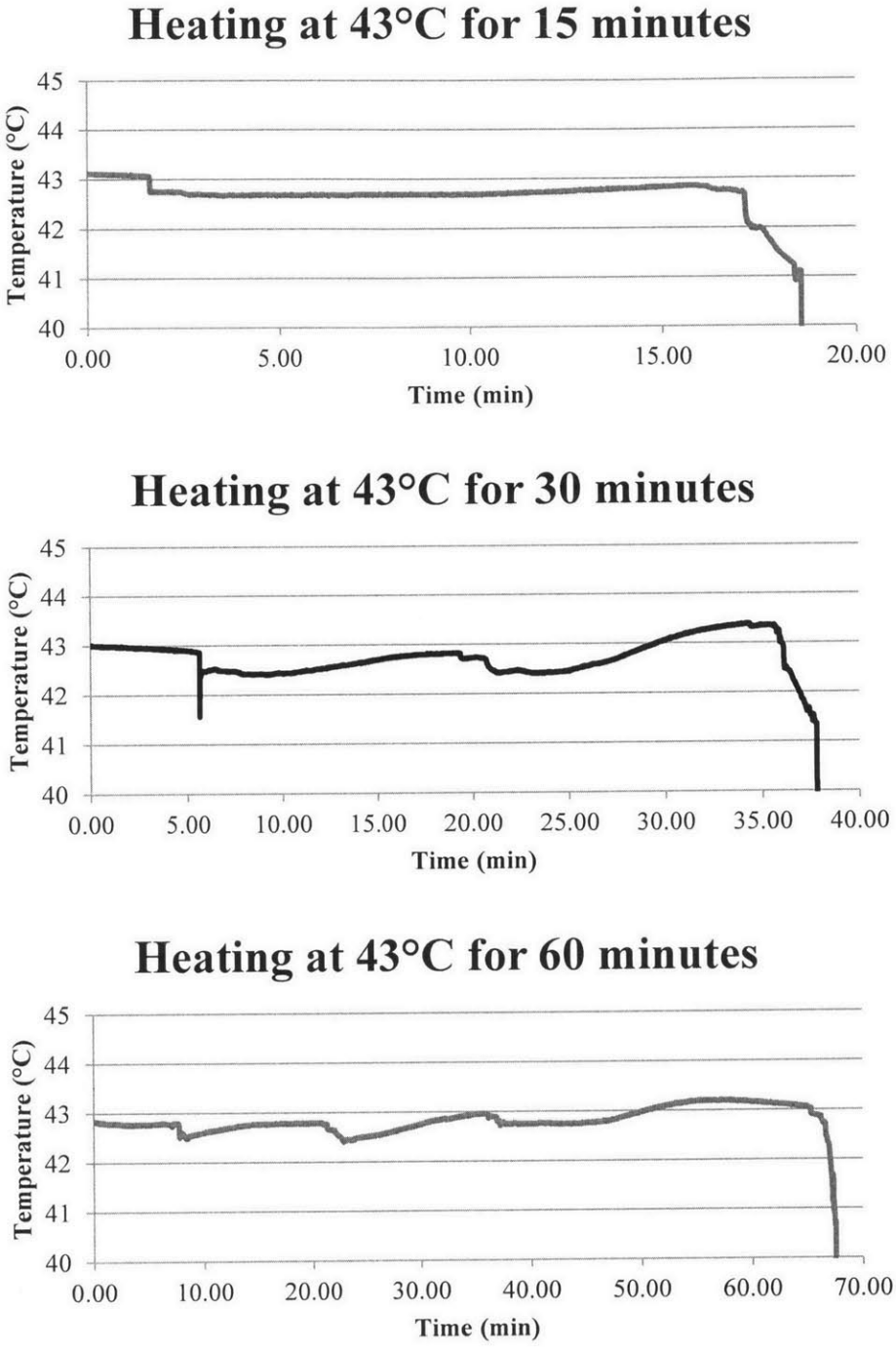

Figure 3-1: Typical examples of heating at 43°C for 15, 30 and 60 minutes. There is a brief decrease in temperature of about 0.25°C when the cells were inserted. In the 30 and 60 minutes experiments, there were similar dips at the 15 and 30 minute timepoints, as cells were removed for lysing. Temperatures during the experiments were within ±0.5°C of the target temperature.

produced. An additional normalization was performed by subtracting the C_T (*Hsp70b* - β-actin) of each timepoint with the unheated control sample C_T (*Hsp70b* - β-actin). To turn the C_T calculations into relative amounts of mRNA, the solution was raised to the power of 2. Standard deviations were calculated from the closest two of the technical PCR

triplicates of each timepoint and propagated through the calculations. The results were graphed and are shown below. Figure 3-2 shows the relative amounts of *Hsp70b* mRNA produced with a heat shock consisting of heating at 43°C for 15 minutes, 30 minutes and 60 minutes durations. *Hsp70b* mRNA production started immediately and peaked at 2 hours for all three durations of heat shock at 43°C. Figure 3-3 shows the average normalized amount of *Hsp70b* mRNA for each of the different heat shocks, organized by heat shock temperature. All of the 43°C and 44°C heat shocks showed the *Hsp70b* mRNA peaking at 2 hours and decaying by 6 hours after the heat shock. The two 45°C heat shocks both showed *Hsp70b* mRNA peaking later, at 4 hours, and decreasing more slowly than the lower temperature heat shocks. In addition, earlier experiments found that *Hsp70b* mRNA production started more gradually for the 45°C heat shocks than the lower temperature heat shocks (data not shown).

Increasing the duration of the heat shocks at the same temperature increased the peak *Hsp70b* mRNA production amounts for heat shock temperatures of 43°C and 44°C. At 45°C, the peak *Hsp70b* mRNA production did not change appreciably when the heat shock duration increased. In contrast, there was a significant difference in the amount of time *Hsp70b* production was increased for heat shocks at 45°C. Heat shock duration did

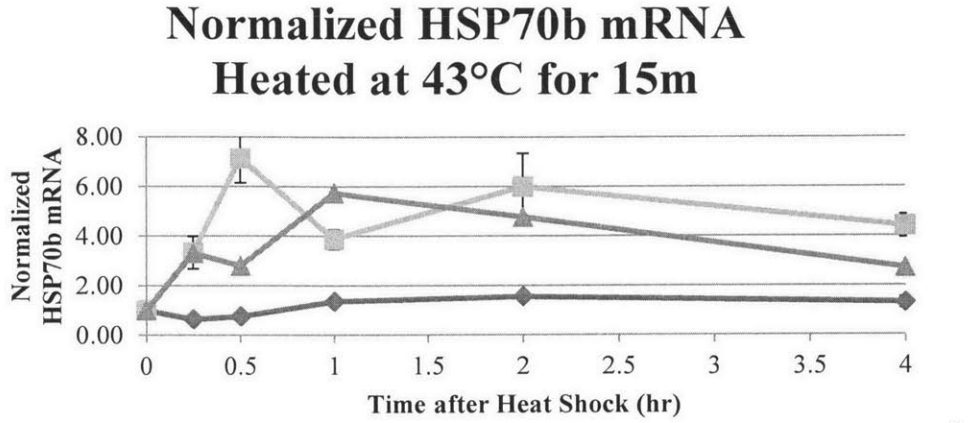

A

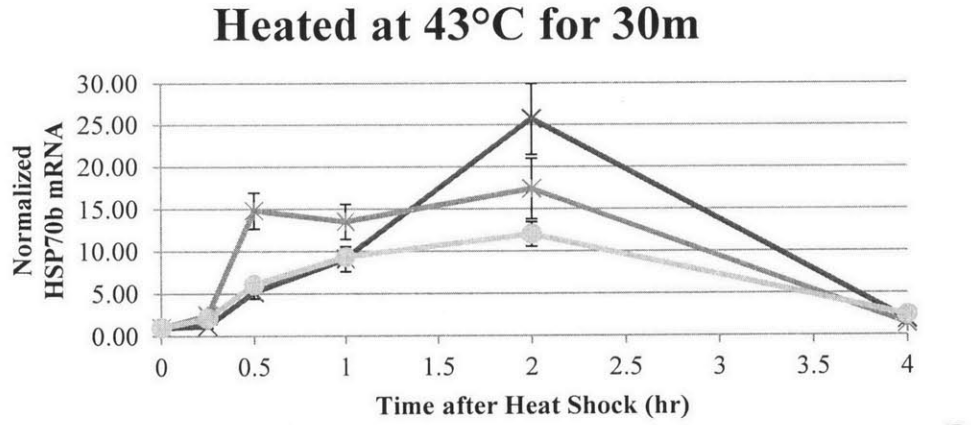

B

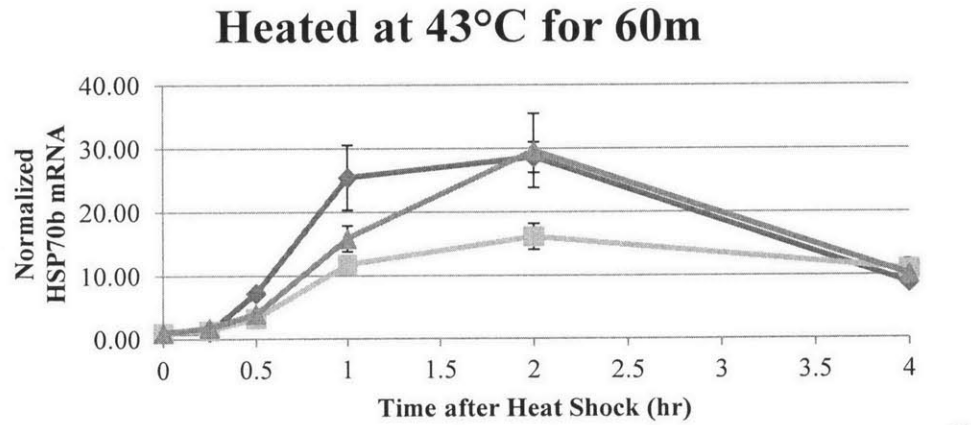

C

Figure 3-2: Normalized HSP70b mRNA production over the 4 hours after heating. Normalized HSP70b mRNA production (calculated from PCR results) of the three individual trials for heat shocks consisting of heating at 43°C for (A) 15, (B) 30 or (C) 60 minutes. The error bars represent the standard deviation due to differences in the technical triplicates.

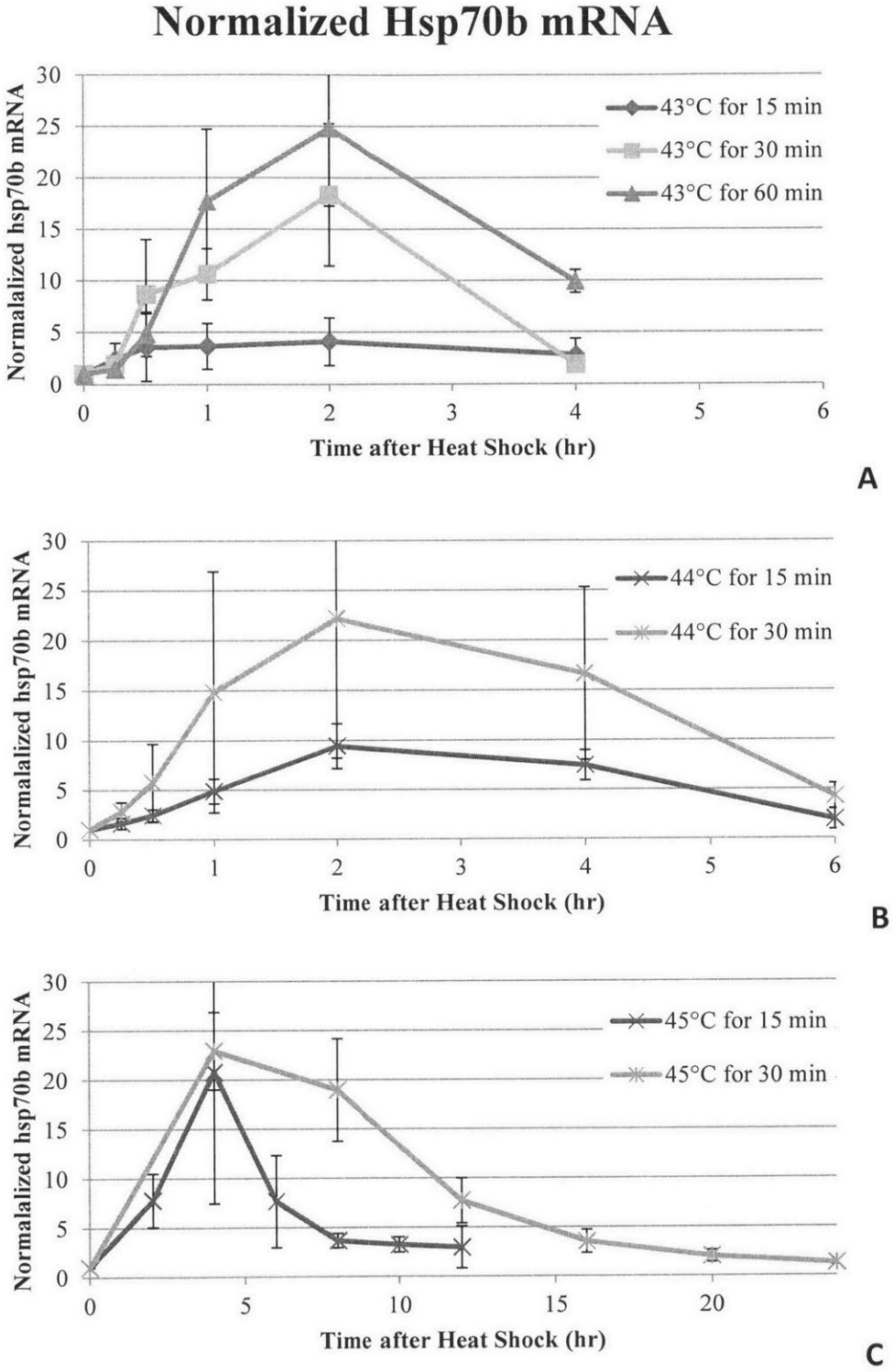

Figure 3-3: Average Normalized Hsp70b mRNA Production after Heat Shock Arranged by Temperature of Heat Shock. Average normalized hsp70b mRNA production after heat shocks at (A) 43°C for 15, 30 and 60 min, (B) 44°C for 15 and 30 min, and (C) 45°C for 15 and 30 min. The error bars represent the standard deviation between experimental samples.

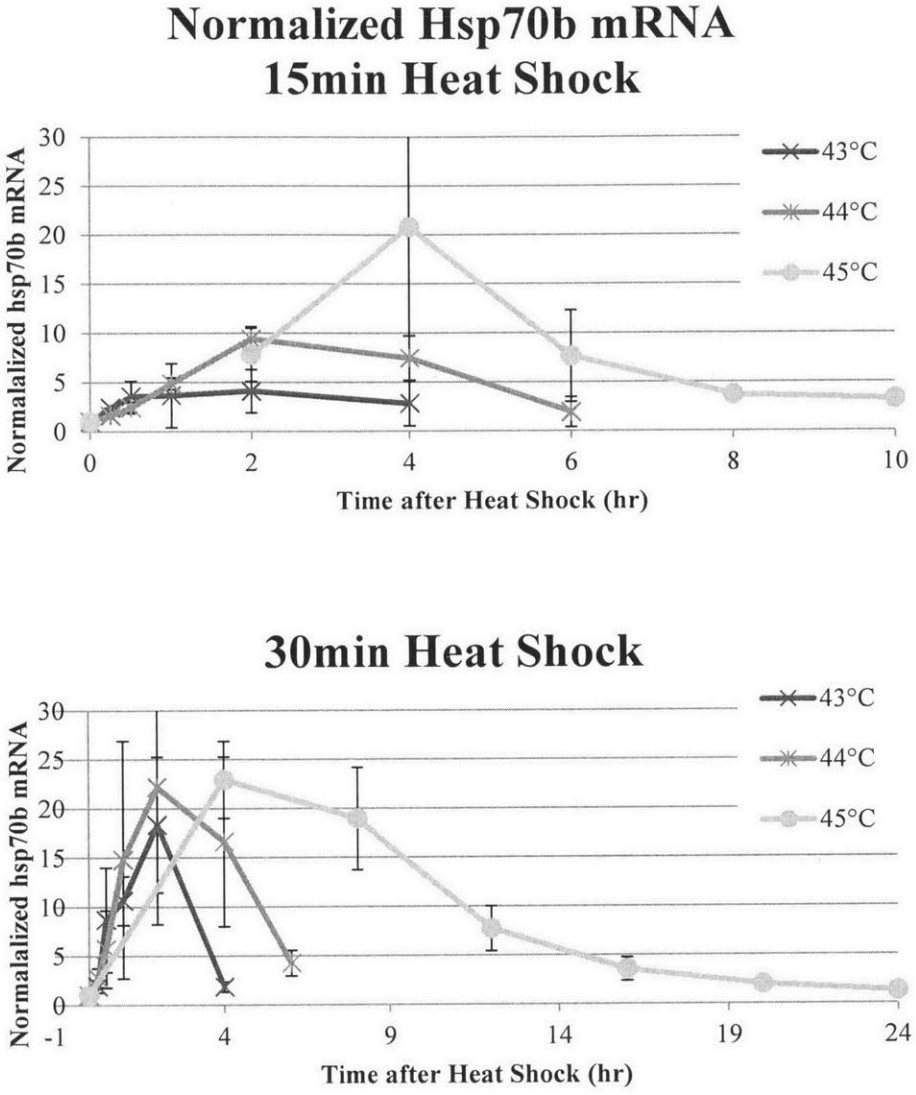

Figure 3-4: Average Normalized Hsp70b mRNA Production after Heat Shock Arranged by Duration of Heat Shock. Average normalized hsp70b mRNA production after heat shocks at (A) 43°C, 44°C, and 45°C for 15 minutes and (B) 43°C, 44°C, and 45°C for 30 minutes. The error bars represent the standard deviation between experimental samples.

not affect the amount of time *Hsp70b* production was increased for heat shocks at 43°C and 44°C.

Grouping the results by duration of heat shock (Figure 3-4) showed that the peak amount of *Hsp70b* mRNA production increased considerably with heat shock temperature when the heat shock duration was 15 min; almost doubling when temperature was increased 1°C. But when the heat shock duration was increased to 30 min, the peak *Hsp70b* mRNA production did not increase appreciably with temperature, particularly with the 44°C and 45°C heat shocks. At both heat shock durations, the amount of time *Hsp70b* mRNA is elevated increased with temperature.

3.4 Discussion

There were several interesting considerations in designing this experiment. First, a fast and consistent method of heating cells was needed. Previous studies generally heat shocked cells by submerging cell culture flasks or dishes into a waterbath heated to the target temperature (Blackburn et al., 1998; Brade et al., 2000, 2003; Gerner et al., 2000). However, temperature monitoring during the protocol design of this experiment, using thermocouples attached to the cell culture plates, showed that plates taken from a 37°C incubator and placed in a 43°C waterbath took over 7 minutes to reach the target temperature. The previous studies referred to above involved 1 to 2 hour duration heat shocks, so the time to target temperature was perhaps not as significant. The 15 and 30 minute duration heat shocks planned for these experiments made that amount of ramp-up time unacceptable, so other methods needed to be explored. Liu et al. plunged cells attached to glass coverslips into heated media (Liu et al., 2005), but that method did not allow enough cells to be heated simultaneously for the desired number of timepoints in these experiments. Other preliminary protocols tried involved using a hot-plate for the

initial temperature increase, then moving the cell culture plates to the waterbath once the desired temperature was reached. Temperature control with that method proved to be difficult. Using the rt-PCR machine to heat the cells in solution was attempted, but as with the glass coverslip method, not enough cells were able to be heated in the same session to allow for a full kinetic analysis of *Hsp70b* mRNA production.

Another study actually used a similar methodology as this paper, trypsinzing and pelleting the cells, then inserting the cells into a centrifuge tube of heated media. That study only used 3 mL of heated media (Vekris et al., 2000). Temperature monitoring in that experiment was done on a "sister tube" that did not have cells inserted, so it is unclear if the insertion of cells caused the temperature of the media to decrease and, if so, how long it took to reach the target temperature again. In this study, by mixing cells in 1 mL of room temperature growth media into 40 mL of heated growth media, the temperature change was either less than 0.5°C or the return to ±0.5°C of the target temperature was less than a minute.

The second major consideration was the selection of genes to be used. Endogenous *Hsp70b* produces less mRNA when heated than an exogenesis *Hsp70b* promoter-reporter gene construct, likely due to multiple copies of gene constructs incorporating into each cell. In addition, it is possible to use an *Hsp70b* promoter specially designed to increase gene translation as mentioned in Chapter 1. However, the reporter gene construct would need to have a control gene construct to normalize measurements. This normalization

presupposes that the two constructs integrate into the cells of every experiment in the same ratio. It was determined that the disadvantage of the normalization assumption required for an exogenous gene construct outweighed the lower mRNA production expected from using endogenous *Hsp70b*.

mRNA was chosen as the parameter to be measured instead of proteins because mRNA expression, as an early measurable quantity of gene transcription, enabled elimination of as many other cellular factors besides heat as possible. Using rt-PCR enabled quantitative measurements of endogenous *Hsp70b* mRNA. The typical protocol for measuring protein production in these types of experiments involved measurements of luminescence produced by a reporter gene such as luciferase or GFP. In addition to the control factors associated with gene constructs as discussed above, luminescence measurements made during preliminary protocol design showed significant variability depending on the speed in which the analysis preparation was performed.

The decision to use mRNA expression did have the drawback of making it difficult to compare results with previous work done by others. Kline and Morimoto looked at mRNA kinetics of *Hsp70* in HeLa cells during and after a 4 hour heat shock at 42°C (Kline and Morimoto, 1997). They found transcription started immediately, peaked 30 minutes after the beginning of the heat shock and returned to basal levels within 2 hours, despite the heat shock being ongoing. That work also showed the initiation of *Hsp70* mRNA kinetics closely followed HSF1 DNA binding, which occurs as HSF1 is

denatured from Hsp90 and forms trimers. Interestingly, the DNA binding declined more gradually than transcription of *Hsp70*. Later work by the same group showed the reproducibility of these kinetics (Jolly et al., 1999). This study examined heat shocks between 43 and 45°C with much shorter durations. Transcription still started immediately, but peak expression occurred later, at 2 hours post-heat shock for the 43 and 44°C heat shocks and 4 hours for the 45°C heat shocks. This suggests that as the temperature of the heat shock increases, the time of peak expression increases as well. In agreement with the Kline and the Jolly papers, *Hsp70b* mRNA expression started to decrease immediately after the peak for all the heat shocks examined. The decline generally did become slower as the heat shock temperature increased.

Tang et al. in 2005 measured *Hsp70b* mRNA kinetics in PC-3 cells heat shocked at 43°C for 1 hour (Tang et al., 2005). They found peak *Hsp70b* mRNA expression occurred at 3 hours, and declined to 20% of the peak expression by 6 hours. The same heat shock in this study found peak expression at 2 hours after heat shock (3 hours after heat shock was not sampled) and expression was at 40% of the peak expression at 4 hours after heat shock.

Several papers have speculated, as in section 2.4 of this paper, that thermal dose may be correlated to *Hsp70b*-promoted protein production since the denaturing of HSF1 from Hsp90 is considered the activating step in Hsp70b production (Liu et al., 2005; Lu et al., 2009). As mentioned in the introduction, thermal dose is a mathematical model that

relates the biologic effect expected at the actual temperature and length of time the tissue is held at that temperature to the amount of time it would take to get the same biologic effect at a given reference temperature. This biological effect is related to the amount of protein denaturation leading to necrosis.

Table 3-1 compares the thermal dose from the varying heat shocks in this experiment with peak *Hsp70b* mRNA (normalized to unheated control) as well as the total amount of *Hsp70b* mRNA (normalized to unheated control) available for translation, which was calculated by integrating the mRNA levels over time. Peak mRNA did not correlate with thermal dose. Instead, there appeared to be a saturation level of *Hsp70b* mRNA. This is in agreement with Lu et al., who also found a saturation level where peak protein levels of the reporter gene *Hsp70b*-GFP eventually stopped increasing with temperature and duration in surviving cells. (Liu et al., 2005).

Thermal dose, on the other hand, did correlate with total *Hsp70b* mRNA available for translation under the conditions used in this experiment. Using the student t-test, total *Hsp70b* mRNA produced during heat shocks of varying temperature and duration but the same thermal dose were statistically insignificant ($p > 0.1$) while heats shocks with varying thermal doses were statistically different ($p < 0.05$). These results are shown in Figure 3-5. The correlation of thermal dose and total *Hsp70b* mRNA using a linear best fit line has an r^2 value of 0.91 (Figure 3-6).

These results suggest the possibility that a model could be developed to predict protein "dose" given detailed information of the heat shock. Deckers at al. recently demonstrated an Arrhenius-type relationship in heat-induced protein expression at 4 hours after heating between 43 and 45°C, albeit with a different heat shock promoter (Deckers et al., 2012). However, modeling the translation process from mRNA to protein is likely to be difficult due to translation efficiency after heat shock, differing stability of the particular mRNA and protein used and the reality of inhomogeneous heating *in vivo*. Heat shock makes translation of mRNA into proteins less efficient. This effect lasts approximately 2 hours.

Table 3-1: Comparison of thermal dose to peak and total *hsp70b* mRNA expression.
The error is the standard deviation between experimental samples.

Thermal Dose (t_{43} equivalent minutes)	Heat shock	Peak mRNA	Total mRNA
15	43°C 15 minutes	4.1 ± 2.3	13.8 ± 3.4
30	43°C 30 minutes	18.4 ± 6.9 †	41.2 ± 8.0 *
	44°C 15 minutes	9.4 ± 2.3 ††	36.0 ± 3.6 *
60	43°C 60 minutes	24.8 ± 7.5 †	62.7 ± 9.4 **
	44°C 30 minutes	22.2 ± 14.0 †,††	84.9 ± 21.0 **
	45°C 15 minutes	20.8 ± 13.3 †,††	90.2 ± 20.5 **
120	45°C 30 minutes	23.0 ± 3.9 †	225.2 ± 19.9

†,††,*,** p-value < 0.05

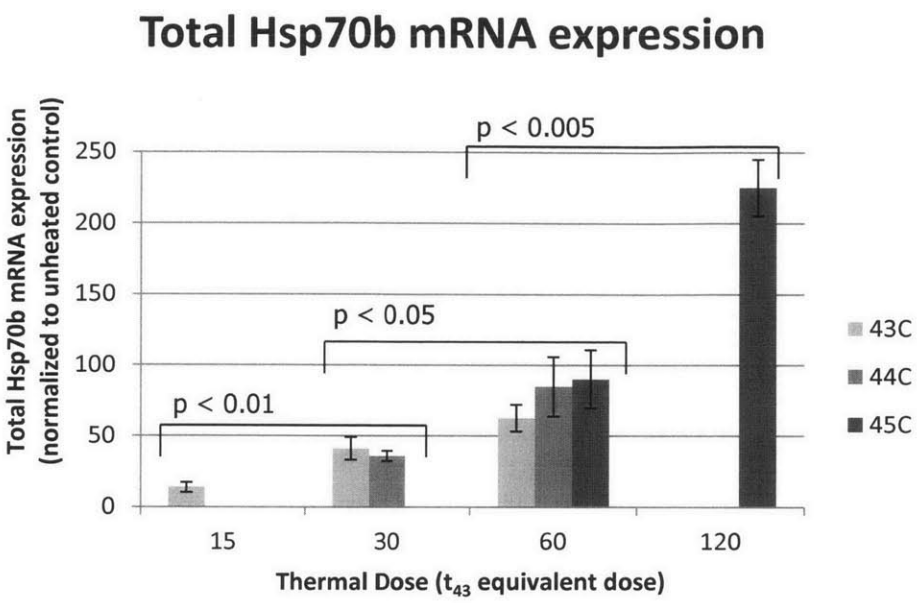

Figure 3-5: Total *Hsp70b* mRNA versus Thermal Dose
Thermal dose correlated with total *Hsp70b* mRNA available for translation under the conditions used in this experiment. Total *Hsp70b* mRNA produced during heat shocks of varying temperature and duration but the same thermal dose were statistically insignificant ($p > 0.1$) while heats shocks with varying thermal doses were statistically different ($p < 0.05$).

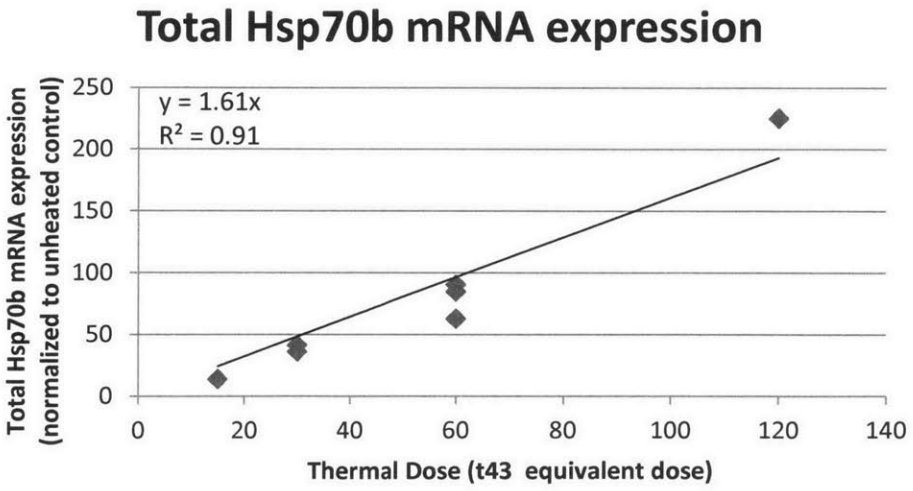

Figure 3-6: Correlation of Total *Hsp70b* mRNA and Thermal Dose
The correlation of thermal dose and total *Hsp70b* mRNA using a linear best fit line had an r^2 value of 0.91. Error bars are omitted for clarity.

The level and length of inhibition differs between cell types (Duncan and Hershey, 1984). This phenomena is less dramatic with HSPs because while the typical CAP-dependent translation is inhibited almost completely, HSPs are preferentially translated through a less efficient CAP-independent pathway (Rhoads and Lamphear, 1995; Yueh and Schneider, 2000). As the results of this experiment showed, *Hsp70b* mRNA often remained elevated longer as temperature and/or duration increased. Accordingly, translation will also increasingly shift to the more efficient translation pathway as temperature and/or duration increase.

The second difficulty in developing a heat-activated gene therapy dosage model is the stability of the mRNA and proteins produced by any particular gene therapy will be dependent on the particular gene used. Previous work in this area generally examines protein kinetics using *Hsp70b* promoters and reporter genes. Studies using *Hsp70b*-GFP constructs generally found that peak protein levels occurred between 16 and 24 hours after heat shock and had mostly dissipated by 72 hours using HeLa, glioma, 4T1 and DU-145 cells (Gerner et al., 2000; Huang et al., 2000; Liu et al., 2005; Vekris et al., 2000). However, studies using *Hsp70b*-βgal genes showed peak protein levels at 3-6 hours and a return to basal levels within 12-24 hours after heat shock (Arai et al., 1999; Blackburn et al., 1998; Brade et al., 2000). Brade also noted that there are considerable differences in the peak level of expression in different cell types. This could suggest that mRNA stability of the reporter gene may be a more important factor in the duration of heat-induced expression, while the peak levels of expression may depend more on cell type.

Finally, hyperthermia *in vivo* is not uniform spatially or temporally. It remains to be seen how significant temperature changes during a single heat shock will affect mRNA and protein production kinetics.

The correlation between thermal dose and *Hsp70b* mRNA production is an indicator that a "dose model" might be possible for heat-inducible promoter gene therapy using focused ultrasound hyperthermia. Chapter 4 examines the feasibility of using waterbath experimentation, where even and consistent temperatures can be maintained, as a substitute for ultrasonic heating in the development of such a model.

4 Comparison of Hsp70b Kinetics in Two Heating Modalities

4.1 Motivation

The correlation between thermal dose and *Hsp70b* mRNA production is an indicator that a "dose model" might be possible for heat-inducible promoter gene therapy using focused ultrasound hyperthermia. The next step was to determine if heating via ultrasound resulted in different *Hsp70b* mRNA kinetics. As *Hsp70b* is considered to be a solely heat activated gene, the mechanical stress due to ultrasound would not be predicted to affect the results. If this was to be confirmed, it would allow simpler and more precise waterbath experiments to be used to build a model of expected protein production given any heating profile. This model could then be applied real-time to MRI temperature mapping during ultrasonic heating to predict the "dose" of gene therapy expected to be produced in the hours and days after treatment.

4.2 Materials and Methods

4.2.1 Construction of Experimental Apparatus

A 15 cm by 15 cm watertight box was constructed of 4 mm acrylic, glued together with 99% 2-Butanone, also known as MEK, (Aldrich Chemical Co, Milwaukee) and made waterproof with silicone (GE, Fairfield, CT). The ultrasound transducer (described in the next section) was fixed to the bottom of box. A second, smaller watertight box (8.5 cm x 12 cm x 12 cm) was suspended 11.5 cm from the bottom of the larger box, 2.7 cm above the focal point of the transducer.

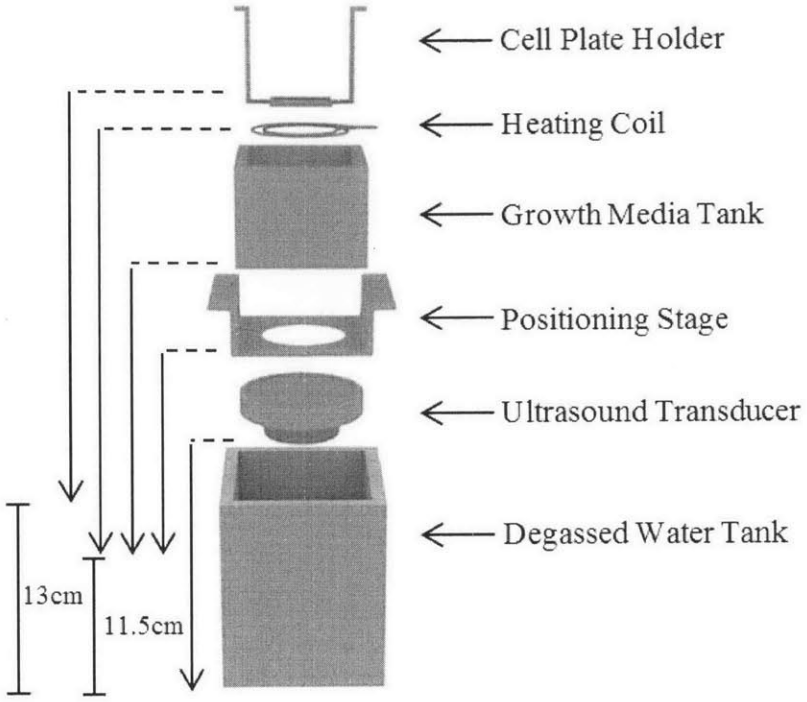

Figure 4-1: Ultrasound Apparatus
The ultrasound transducer was placed in a 15 x15 x 15 cm acrylic tank of degassed water. A second, smaller tank (8.5 cm x 12 cm x 12 cm) with a Mylar bottom was suspended 11.5 cm from the bottom of the larger box, 8.2 cm from the center of the transducer. A heating coil carrying heated water was used warm a solution of 1:1 Growth Media:PBS. Cells attached to a Mylar cell plate (Figure 4.2) were suspended in the second box 13 cm from the bottom of the transducer.

The sides of this smaller box were also constructed of 4 mm acrylic. However, the bottom was made of 0.03 mm ultrasonically translucent Mylar. The smaller box was constructed to fit together more tightly, using MEK to make the box as watertight as possible. This was because it was discovered the silicone was toxic to the cells used in the experiments. Silicone still had to be used to ensure the box was waterproof, but it was spread on the outside joints of the box to prevent as much contact of growth media with silicone as possible.

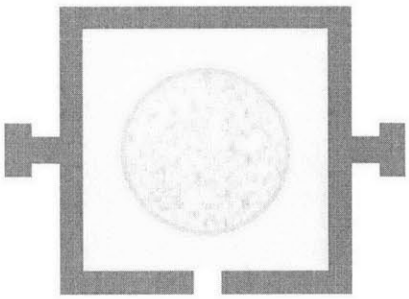

Figure 4-2: Cell Plate Design
A 5 cm by 5 cm by 4 mm frame (dark gray) holds a 0.03 mm thick sheet of Mylar (light gray), which the cells are grown upon. Cells outside a 12 mm radius circle centered in the cell plate were removed prior to heat shock. A channel in the frame eliminated air bubbles during placement in the tank.

The Mylar bottom of the smaller box allowed the majority of the ultrasonic pathway to be in deionized and degassed water, which filled the larger box, including the focal point (8 cm from the center of the transducer). A 1:1 solution of growth media and PBS filled the smaller box.

Cell plates were constructed of the same 0.03mm thick Mylar, held sandwiched between thin frames of 2 mm acrylic. The frames were held together by MEK, but no silicone due to the toxicity mentioned above. During the experiments, the cell plates were centered and suspended in the smaller box 2.5 cm from the bottom, putting the plates 10.7 cm above the center of the transducer. An ultrasound absorber, made of 8 mm thick rubber, was suspended at a 45 degree angle in order to direct any ultrasound waves not absorbed away from the cell plates.

Heating the growth media/PBS solution was accomplished through the use of a copper heating coil. Water from a heated water bath was pumped through the coil to warm the growth media/PBS solution. In order to ensure an even temperature distribution, the

entire apparatus was placed on a rotator (Belly Button, Stovall, Greensboro), set to 36 rotations/minute. This was necessary because placing each cell plate into the growth media disrupted the solution. If the apparatus was still, there were severe temperature gradients present, both from the heating coil as well as the sides of the box. When the solution was disrupted by the placement of the cell plate, there was a significant change in temperature of several degrees at the cell plate location. The rotator caused constant mixing of the solution, reducing any temperature gradients so there was little temperature disruption when the cell plates were put in place. Three thermocouples were used to monitor the temperature during the experiment. One was placed in the degassed water, away from the ultrasonic pathway. Another was placed in the growth media tank, at the height of the cell plates, but also out of the ultrasonic path. A third, made of bare-wire, was attached to the cell plate arms, close to the cell plate. This third thermocouple was intended to determine how fast the cell plate heated after being placed into the heated solution. Although not directly in the ultrasonic path, its placement was closer than the others, and therefore a copper-constantan bare-wire thermocouple was used to minimize measurement artifacts (Hynynen and Edwards, 1989) and prevent an additional source of heat near the cells. The bare-wire thermocouple was constructed in-house of 50μm diameter copper and constantan wire (California Fine Wire Co., Grover Beach, CA) connected by soldering.

4.2.2 The Ultrasound Transducer

The experiments were performed with an in-house manufactured, single-element, spherically curved, air-backed piezoceramic transducer. It had a diameter of 10 cm and

an 8 cm radius of curvature. The experiments were run at the transducer's resonant frequency of 1.653 MHz. An external matching box (also manufactured in-house) containing an inductor-capacitor circuit was constructed to make the electrical impedance of the transducer 50 Ohms.

The ultrasound driving signal was generated via a function generator (Fluke 396 125Ms/s Arbitrary Waveform Generator, Mississauga, Canada). The signal was amplified with an RF Power Amplifier (E&I, Rochester, NY). Power measurements were performed with a RF power meter (Bird, Solon, OH).

The transducer efficiency was measured using an acoustic radiation force balance system (Hynynen, 1993). The transducer was immersed in degassed and deionized water. With the same equipment used in the experiments, the transducer was driven between 0.02 and 0.12 $V_{p\text{-}p}$ in 40 mV steps. A densely bristled brush (constructed in-house) was arranged opposite to the transducer, enabling absorption of the complete acoustic beam, with the focal point of the transducer located inside the brush.

The brush was suspended in the water by thin wires attached to an electronic weight balance (XS205 Dual Range, Mettler Toledo, Columbus OH). For each voltage step, electric power was recorded and acoustic power calculated from the force exerted on the brush with the following equation

$$P_{Acoustic} = {}^{m \times g \times c}/_{\cos(\theta)}$$

where m is the change in weight of the absorbing brush during sonication, c is the speed of sound in water, g is the gravitational constant 9.81 m/s^2 and θ is the angle of incidence of the transducer. To compute the efficiency of the transducer, the output acoustic power was divided by the input electrical power for each step and averaged (Table 4-1).

Using a 0.4 mm diameter needle hydrophone (ONDA, Sunnyvale, CA), measurements of the acoustic intensity produced by the transducer were made at the focus. The signals were recorded by a Tektronix TDS 380 oscilloscope (Beaverton, OR) and stored on a personal computer using software written in Matlab (Mathworks; Natick, MA). The

Table 4-1: Acoustic efficiency of air-backed single-element transducer. Frequency: 1.653 MHz; Radius of curvature: 80 mm; Diameter: 100 mm; F number: 0.8.

Voltage (V)	$P_{electric}$ (W)	$P_{acoustic}$ (W)	$\frac{P_{acoustic}}{P_{electric}}$
0.04	0.08	0.05	66%
0.08	0.34	0.21	62%
0.12	0.77	0.46	60%
0.16	1.36	0.81	60%
0.20	2.15	1.32	62%
0.24	3.05	1.88	62%
		Average	62%

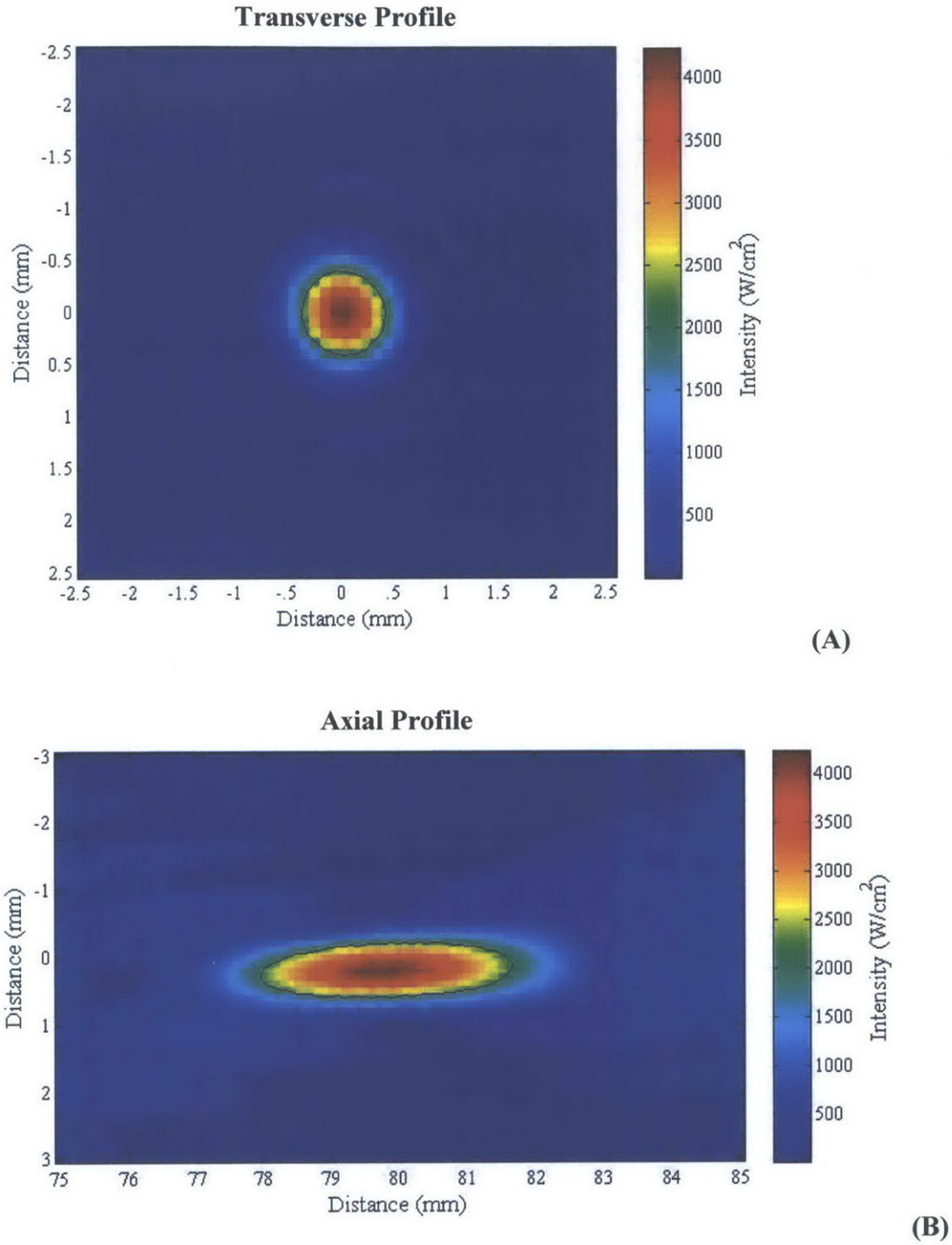

Figure 4-3: Beam Plots of the Focal Area.
Characteristic Beam Plots of Acoustic Intensity. (A) A 5×5 mm transverse profile, centered at the focus. (B) A 6×10 mm axial profile, centered at the focus. Scans were performed with 0.1 mm steps. The black circles represent the full-width half-maximum width and length of the focal region

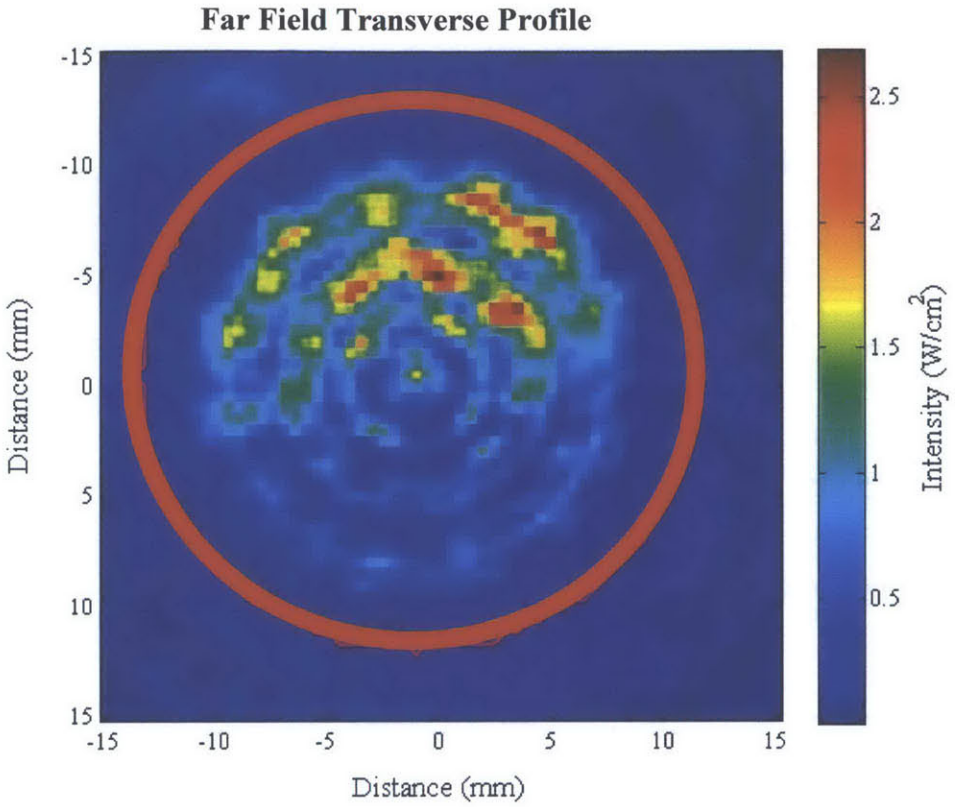

Figure 4-4: Beam Plot of the Cell Plate Plane
A 30×30 mm transverse beam plot performed with 0.5 mm steps, centered at the level of the cell plate (10.7 cm from the center of the transducer). The red circle represents the area in which cells were attached during the experiment.

transducer was immersed in degassed, deionized water facing the tip of the hydrophone. The water tank was lined with rubber, an ultrasound absorbing material, to reduce interference. Axial and transverse profiles (beam plots) of the focal area were measured (Figure 4-3) as well as a transverse profile in the area that the cell plate sits in the experiments (Figure 4-4). The full-width half-maximum width and length of the focal region in the intensity scans were 3.7 and 0.8 mm in the axial and transverse directions, respectively.

The experiments described in this chapter used an acoustical power of 32 W. The peak acoustic intensity at the focus was 4243 W/cm^2, while the average acoustic intensity over the -3dB isointensity contour was 3103 W/cm^2 in the transverse plane and 3086 W/cm^2 in the axial plane. In the transverse plane of the cell plate (10.7 cm from transducer center), the peak acoustic intensity was 2.7 W/cm^2, and the average acoustic intensity over the 24 mm circle in the far-field that contained the cells was 0.60 ± 0.47 W/cm^2.

4.2.3 Ultrasound Power Selection

The power used during the experiments was selected by heating a human-tissue mimicking phantom with various power levels to find one that reached a minimum of 43°C over a 12 mm radius circle centered 2.6 cm distally from the focus. The far-field of the ultrasound beam was used to heat a wide area without having to steer the focal point. The phantom was made using the method described by Madsen in 1998, with the exception of using penicillin/streptococcus (Gibco) in the place of thimerosal (Madsen et al., 1998).

It was found that setting the ultrasound to 50W (electric) caused copper-constantan bare-wire thermocouples set at 0mm, 4mm, 8mm, 10mm, and 12mm from the center of the focus to record temperatures of at least 43°C (Figure 4-5). As 50W (electric) was at the upper limit of the transducer's capacity and the thermocouples placed farther from the center were measuring temperatures greater than 44°C, meaning most of the circular area

was heated above 44°C, it was decided that this power level would be used for experiments testing heat shocks at both 43 and 44°C.

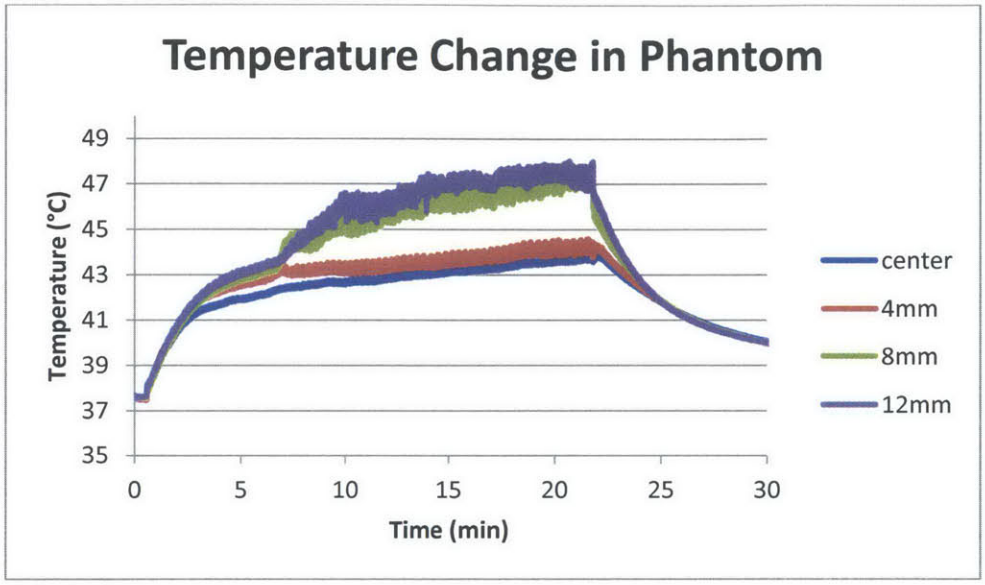

Figure 4-5: Temperature Change in Tissue-Mimicking Ultrasound Phantom. At 50W of power, 4 bare-wire thermocouples arranged from the center of the focus to 12mm away all reached a minimum of 43°C over 15 minutes.

To ensure that the ultrasound did not affect the temperature of the Mylar cell plates at that power level, bare-wire thermocouples were attached to a cell plate in the same configuration as above (0, 4, 8, 12 mm from the center of the focus). The plate was put in the ultrasound apparatus and filled with room temperature distilled water. The water was not degassed because the Growth Media/PBS solution to be placed in the smaller tank during the experiments would not be degassed. The bottom chamber was filled with distilled and degassed water. There was no change in temperature, all probes measuring 22.6°C with a standard deviation over the 40 minutes of ultrasound exposure of less than 0.15°C.

4.2.4 Cell Growth

HeLa cells were grown on 15cm tissue culture plates. Growth media was made with 500mL DMEM media (Gibco) containing 2.75mg glutamine (Gibco) supplemented with 50mL fetal bovine serum (BioWhitaker), 50,000 units of penicillin (Gibco) and 50mg of streptococcus (Gibco). The cells were incubated in a Revco Ultima 37°C humidified chamber set at 5% CO_2. Cells were harvested for experiments at 90% confluence.

Two or three days before the experiment, the plated HeLa cells were detached from the plates using 2mL of .25% Trypsin-EDTA (Gibco) per plate. 10 mL of growth media was used to neutralize the trypsin after 5 minutes. Specially built Mylar cell plates (described above) were set into new 15 cm tissue culture dishes (3 plates per dish) with 40 mL of growth media. 1 mL of the cell suspension was then distributed in drops around each of the three Mylar plates in the dish. A total of three tissue culture dishes and nine cell plates were prepared per experimental session. The tissue culture dishes were stored in a Revco Ultima 37 °C humidified chamber set at 5% CO_2 until moved to the ultrasound lab, where they were stored in a Thermo Electron Corporation NAPCO Series 80000 humidified incubator, also set at 37°C and 5% CO_2.

4.2.5 Heating Protocol

Three heat shock temperature conditions were tested; 37, 43 and 44°C. The first condition, 37°C, was chosen to test if mechanical stress alone could cause activation of Hsp70b, in the absence of heat shock. The latter two were chosen to compare with the

waterbath experiments from Chapter 3 and to test if mechanical stress affected the activation of Hsp70b in the context of a heat shock.

On the day of the experimental session, the ultrasound apparatus was set up. The circulating water-tank was set to the appropriate temperature (between 46-48°C depending on ambient temperature and the heat shock temperature being tested). The thermocouple probes were calibrated with a finely graded glass thermometer. With the ultrasound transducer firmly clamped to the bottom of the larger tank, it was filled with deionized and degassed water. The platform and smaller tank were placed in position, taking care to eliminate any bubbles on the Mylar bottom surface. The upper tank was filled with a mixture of 1:1 growth media and PBS (Gibco). To ensure the tank was centered correctly, the ultrasound was briefly turned on when the solution was at the level of the cell plates.

The copper heating ring was placed in the upper tank, along with the cell plate arms and the ultrasound-absorbing rubber bumper. Sterilized thermocouple probes were placed in each tank, out of the way of the ultrasound beam. A bare-wire thermocouple was attached to one of the cell plate arms. The rotator was turned on and set to 36 rotations per minute. The growth media in the upper tank was heated to the desired experimental temperature via the heating coil, utilizing the pump settings to manually control temperature.

When the experiments were ready to begin, the power amplifier was turned on to warm up. One cell plate was removed from the incubator. Using a template, cells outside of a 12 mm radius circle centered on the cell plate were scraped off. Briefly turning the rotator off, the rubber absorber and the cell plate arms were removed from the tank. Then the temperature recording was started, the cell plate was attached to the cell plate holder arms and inserted into the Growth Media tank, and the rubber absorber was put back in place. The rotator was then turned back on to 36 rotations per minute. Next, the ultrasound was turned on using the function generator set at a continuous sinusoid with a frequency of 1.653 MHz, for 15 minutes. The heating coil pump was manually adjusted throughout the 15 minutes to maintain the temperature within ±0.5°C of the desired temperature. After 15 minutes, the ultrasound was turned off. The cell plate was removed from the tank, placed in a 10 cm tissue culture dish with fresh growth media and returned to the 37°C incubator. Another cell plate was taken from the incubator and the same procedure repeated without the ultrasound being turned on. Each experimental session consisted of a total of 4 pairs of cell plates (one heated and sonicated, one just heated) and 1 unheated control cell plate that was left in the incubator.

4.2.6 Analysis

The cells on each cell plate were lysed at one of the experimental timepoints being tested (1, 2, 4 and 6 hours after the heat shock commenced) according to the standard procedure described in the RNeasy Mini Kit (Qiagen) using a QIAshredder. The suspension was mixed with 350μg RNase-free 70% ethanol (Sigma-Aldrich; St. Louis, MO) and stored at

-20°C until the RNA could be isolated. 2μg of RNA was used to make cDNA using a High Capacity cDNA Reverse Transcription kit (Applied Biosystems).

The relative amount of *Hsp70b* DNA in each cDNA sample was quantified using RT-PCR with β-actin acting as the control. The primers used were the same as described in the waterbath experiments in Section 3.2.4.

FastStart Universal SYBR Green Master Mix (Rochc) was used for the florescence dye, nucleotides and Taq DNA polymerase needed for the RT-PCR reaction. Each experimental sample was tested in triplicate. A disassociation curve was produced during each RT-PCR test to check for dimers.

4.3 Results

As mentioned in section 4.2.5, temperature was monitored during all experiments with a TC-1000 Thermometer (Sable Systems International, Henderson NV). Figure 4-6 shows two typical examples; both were 15 minute heat shocks at 44°C. The upper graph shows an experiment with ultrasonically-induced mechanical stress and the lower graph is from an experiment with the ultrasound turned off. The probe on the cell plate holder was inserted into the tank with the cells, showing a fast increase to the desired heat shock temperature of less than 30 seconds. Due to the probe being attached to the thicker acrylic of the arm, it is likely that the cell layer attached to the much thinner Mylar of the cell plate reached the target temperature at a comparable time or faster. Because the bare-wire

probe on the cell plate holder was noisy at times, the pump adjustments to maintain temperature to ±0.5°C of the target temperature were made using the probe situated in line with the cell plate in the growth media tank.

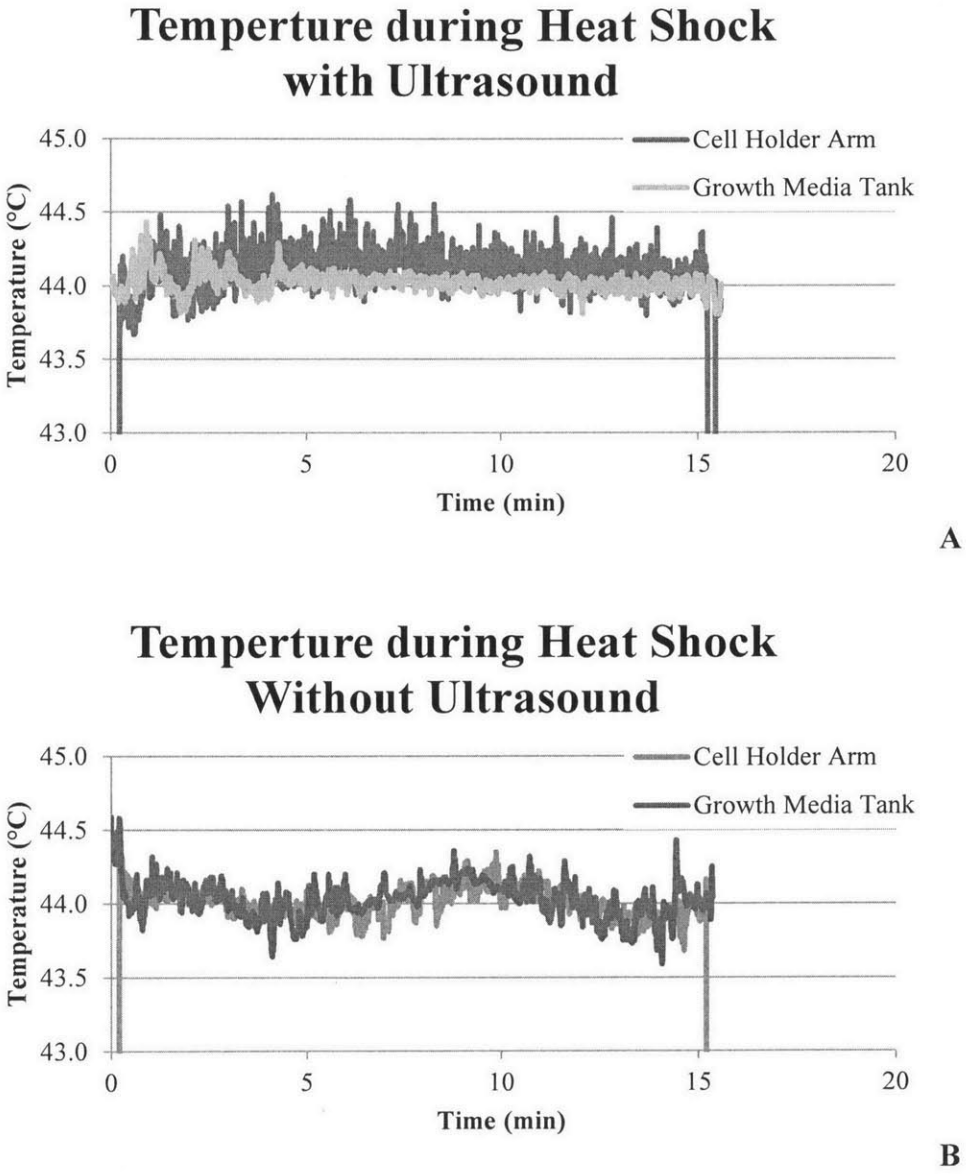

Figure 4-6: Typical Temperature Profile During Heat Shock.
Representative examples of temperature changes during a heat shock. (A) A 44°C heat shock lasting 15 minutes with ultrasonic mechanical stress and (B) without ultrasonic mechanical stress.

Just as in the waterbath experiments, the concentration and purity of all RNA samples were tested with a SmartSpec Plus spectrometer (Bio-Rad; Waltham, MA). Concentrations were generally lower than in the waterbath experiments, due to the limited size of the cell plates. At times, the cells would detach from the plate during the experiment, which also lowered the RNA concentration, sometimes to unusable levels. Purity, defined by the A260/A280 rating, stayed in acceptable levels (1.5-2.0) for all heat shock samples with usable concentrations.

To determine the relative concentration of *Hsp70b* mRNA produced, the isolated RNA was converted to cDNA and rt-PCR was performed, measuring both β-actin and *Hsp70b* cDNA levels. C_T numbers were calculated with a common threshold level of 0.8.

To normalize the amount of cDNA in each sample, the C_T of β-actin was subtracted from the C_T of *Hsp70b*. This allows the cDNA to be directly related to the amount of mRNA produced. An additional normalization was performed by subtracting the C_T (*Hsp70b* - β-actin) of each timepoint with the unheated control sample C_T (*Hsp70b* - β-actin). To turn the C_T calculations into relative amounts of mRNA, the solution was raised to the power of 2.

Figure 4-7 shows mechanical stress did not cause detectable amounts of activation of *Hsp70b* mRNA in the absence of heat shock. Cells were put in the ultrasound apparatus

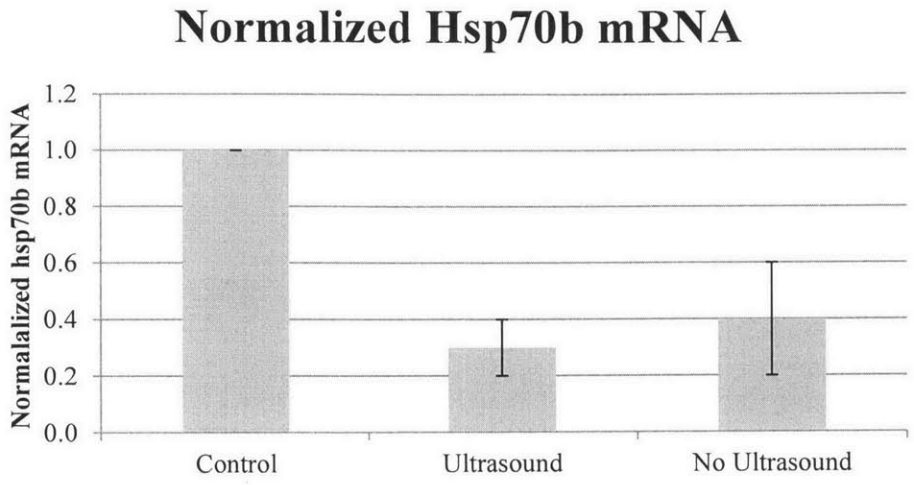

Figure 4-7: Hsp70b Activation Due to Mechanical Stress.
Hsp70b activation after cells were put in the ultrasound apparatus and either exposed or not exposed to ultrasound at 37°C. The control sample was left in the incubator until lysed.

and either exposed or not exposed to ultrasound at 37°C. The cells were then lysed 2 hours later. The control sample was left in the incubator until lysed.

All the sonicated and un-sonicated samples produced less *Hsp70b* mRNA than the control sample, which was grown on a Mylar cell plate like the others but left in the incubator and lysed between the experimental samples.

As explained in Section 4.2.5, experiments were done in pairs to reduce any error introduced by external conditions. Each pair consisted of samples treated with the same heat shock temperature and duration and lysed at the same time after heat shock. One of

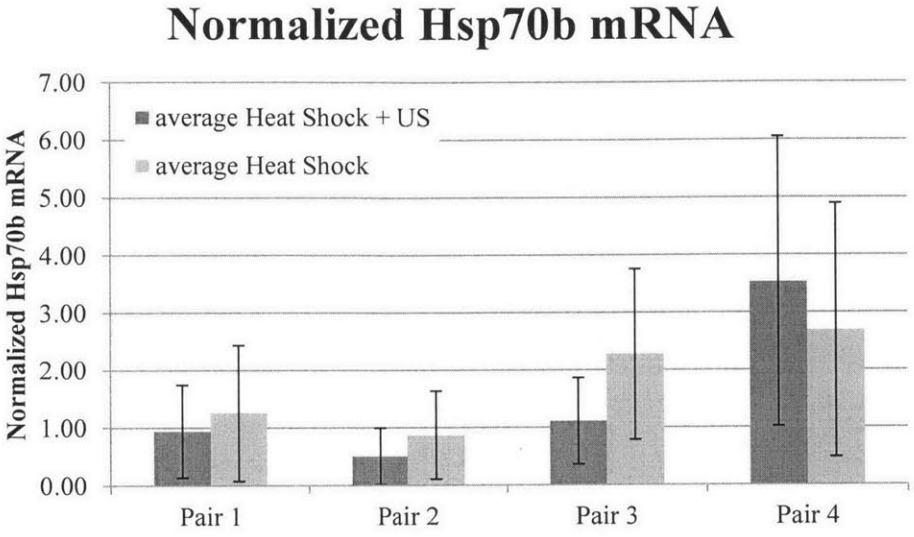

Figure 4-8: Normalized Hsp70b mRNA for Four Experimental Pairs. Four experimental pairs subjected to heat shock at 44°C for 15 minutes. The dark gray bars show normalized hsp70b mRNA amount for the samples that were sonicated during the heat shock. The light gray bars show normalized hsp70b mRNA amount for the samples that were only subjected to heat shock. All samples were lysed at 4 hours after the beginning of the heat shock. The error bars represent the standard deviation of the triplicate samples used during rt-PCR analysis.

each of the pairs was subjected to sonication plus heat shock and the other was subjected to the heat shock alone.

Figure 4-8 shows four of these experimental pairs subjected to heat shock at 44°C for 15 minutes. All samples were normalized to the unheated and nonsonicated control sample from the day of the experiment. The dark gray bars show normalized *Hsp70b* mRNA levels for the samples that were sonicated during the heat shock. The light gray bars show normalized *Hsp70b* mRNA levels for the samples that were only subjected to heat shock. All samples were lysed 4 hours after the beginning of the heat shock. There was no

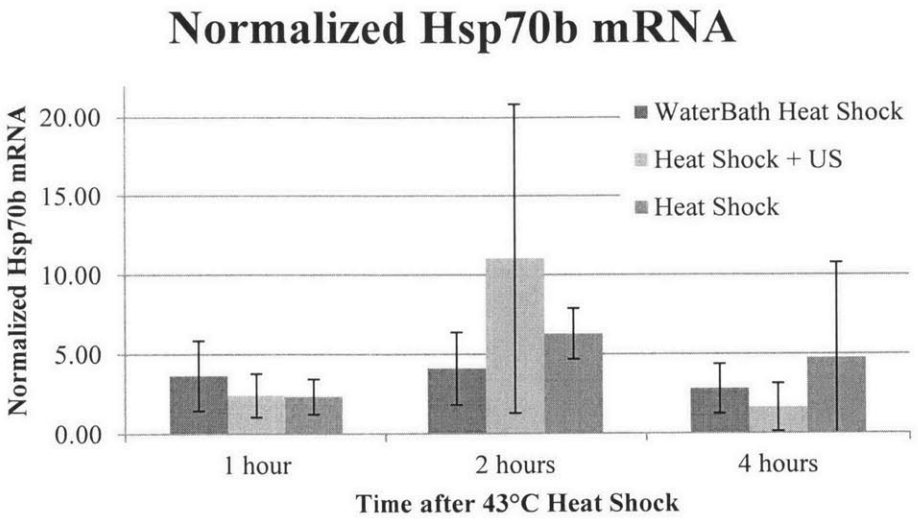

A

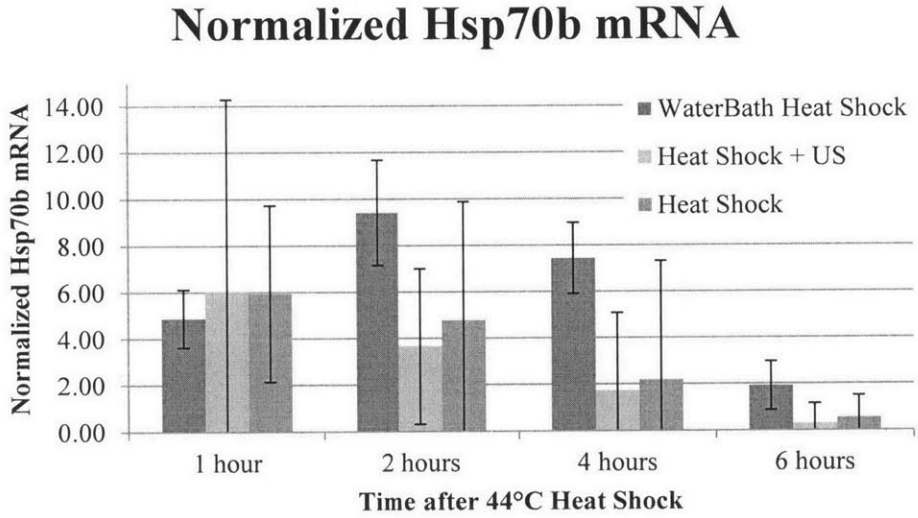

B

Figure 4-9: Comparison of Hsp70b mRNA Levels Over Time
Comparing normalized hsp70b mRNA of cells exposed to various types of 15 minute heat-shocks at (A) 43°C and (B) 44°C. The waterbath heat-shock mRNA levels are from Chapter 3.3. The error bars represent the standard deviation between experimental samples. There was no statistically significant difference between the ultraaound+heat shock samples and the heat shock only samples at any of the timepoints tested ($p > 0.4$). There was also no significant statistical difference between the mRNA levels in the waterbath experiments of the previous chapter and samples tested in this chapter with the same type of heat shock and lysed at the same time after heat shock ($p > .05$).

statistically significant difference in hsp70b mRNA levels between the samples that were sonicated while heat-shocked and those that were only heat-shocked.

Normalized mRNA levels between the different types of heat-shocks at varying times after heat shock were compared (Figure 4-9). As in Figure 4-8, there were no statistical differences between sonicated and nonsonicated samples for either of the heat shocks at any of the timepoints after heat shock tested ($p > 0.4$). The waterbath samples from Chapter 3.3 were also included for comparison. The mRNA levels were statistically equivalent at all timepoints ($p > 0.05$).

4.4 Discussion

The feasibility experiments detailed in Chapter 2 demonstrated the difficulty of predictable, spatially even heating *in vivo*. This is true whether ultrasonic heating is used or another modality due to perfusion changes, movement and other factors. The thermal dose model was developed, among other reasons, to be able to compare *in vivo* studies of hyperthermia (Sapareto and Dewey, 1984). *In vitro* studies using ultrasound-induced heating allowed more predictable heating but are still uneven spatially, causing a ±3°C temperature difference within in a 10 μL PCR tube (Liu et al., 2005). Preliminary experiments for this study attempted to grow cells on a human-tissue mimicking phantom so ultrasonic heating could be instead of a waterbath heat shock. However, as Figure 4-5 from the ultrasonic power selection shows, the temperature differences across a 12 mm distance were up to 4°C.

Developing a predictive model of *Hsp70b*-promoter kinetics would be difficult under those conditions. Ideally, experiments would consist of instantaneous temperature changes and no deviations from the target temperature throughout the duration of the heat shock. Waterbath experiments are much closer to this ideal than ultrasound-induced heating. However, ultrasound causes hyperthermia through absorption of mechanical energy rather than simple heat transfer. Molecules vibrate as the ultrasonic pressure wave transverses tissue, producing heating via friction and other effects. Structural factors of the tissues also affect ultrasonic attenuation. Zhang et al. found the ultrasonic nonlinearity parameter b/a changed with a variety of structural features (Zhang et al., 1991). The effect was greatest with changes in cell to cell adhesion and cell structure. Therefore, it needed to be determined if results from waterbath experiments would be consistent with ultrasonic heating, despite the lack of mechanic stress. If so, a predictive model based on empirical data from waterbath experiments would also be valid for use in ultrasound-induced heating.

In vitro studies to date have looked at mechanical stress activation of Hsp70 have sonicated cells suspended in solution (Hundt et al., 2007; Liu et al., 2005). These works only tested the effect of mechanical stress due to intercellular vibration. Cells generally change shape when attached to a surface. By using cells attached to each other and to the Mylar cell plates in this study, the mechanical stress due to cell to cell adhesion and cellular structure could also be tested as an activation parameter of Hsp70b.

The first set of experiments in the present study tested if mechanical stress caused by ultrasound alone could activate Hsp70b. The amount of *Hsp70b* mRNA from samples sonicated in a 37°C waterbath and lysed 2 hours after heat shock showed no statistical difference from the amount of *Hsp70b* mRNA from samples transferred to the 37°C waterbath but not exposed to ultrasound. Both conditions showed reduced levels of *Hsp70b* mRNA compared to a sample left in the incubator throughout the experiment, which suggests the experimental protocol itself might have caused some biological stress.

Even if mechanical stress cannot cause activation of *Hsp70b* alone, it could increase or inhibit activation during a heat shock. To ensure even and consistent heating between samples, the heat shock was supplied with a circulating waterbath. By testing the temperature rise in a human-tissue mimicking ultrasound phantom, an acoustic power was chosen that caused the phantom to heat to at least the target heat shock temperature in the sample area. By using the same power on cells attached to the Mylar cell plates, the cells were exposed to the same amount of mechanical stress without additional heating. It is possible that intercellular vibrations could have caused some local temperature change, but the cells were plated in a monolayer, so the circulating waterbath would likely dissipate any extra heat quickly.

For 15 minute heat shocks at 43 and 44°C, there were no statistical differences in the amount of *Hsp70b* mRNA between samples which were sonicated and those that were not at any of the timepoints tested ($p > 0.4$). There was also no significant statistical

difference between the mRNA levels in the waterbath experiments of the previous chapter and samples tested in this chapter with the same heat shock and lysed at the same time after heat shock, although the p-value was smaller ($p > .05$).

This study had several limitations. Although this is the first *in vitro* study to examine mechanical stress on attached cells, the cells were still arranged in a monolayer on a synthetic surface. The response of cells in tissue could differ from cells on a monolayer. Liu et al. looked at Hsp70b activation due to ultrasound-induced mechanical stress caused by cavitation alone *in vivo* and found a 4-fold increase in the reporter protein expression versus a 170-fold increase caused by a ultrasound-induced hyperthermia protocol designed to reduce cavitation (Liu et al., 2006). It also should be noted that, in this study, the standard deviations of the mRNA expression between samples were quite high. This could be due to a variety of factors as the 3 sets of paired experiments at each heat shock condition were often tested on different days, which also meant the mRNA isolation was performed on different days. A variety of factors (average temperature, ultrasonic power, time of experiment, mRNA purity) were examined for patterns in the expression levels, but no correlations were found.

Based on the results of this study, we can conclude that waterbath experiments are an acceptable substitution for ultrasound in the development of a predictive model for *Hsp70b*-promoted gene therapy activated by ultrasonically-induced hyperthermia.

5 Conclusions and Recommendations for Future Work

The long-term goal of this research is to control effective gene therapy delivery spatially, temporally and dosing. Chapter 2 showed the feasibility of spatially and temporally controlling a heat-induced reporter gene using ultrasound-generated hyperthermia guided with MRI temperature mapping in a large animal model, the first study of its kind. Chapter 3 analyzed the reproducibility of mRNA kinetics for a variety of strictly defined heat shocks and found a relationship between thermal dose and total *Hsp70b* mRNA production. Having shown that the possibility of developing a predictive mathematical model of therapeutic dosing using a heat-induced promoter gene therapy construct, chapter 4 found that mechanical stress alone did not activate Hsp70b. Since there was no statistical difference between *Hsp70b* mRNA production using waterbath experiments versus ultrasound experiments, the development of the predictive dosing model does not need to depend on ultrasonic experiments. As this work has shown, *Hsp70b* mRNA kinetics can change dramatically with just a 1°C difference in the delivered heat shock. Designing a predictive model will require precision control of temperature and duration of heat shock, which is difficult using ultrasonic heating. Once this predictive model is made, however, it can be deployed in real-time using minimally invasive ultrasonically-induced hyperthermia with MRI temperature mapping in the same way ultrasonic surgery currently predicts extant of necrosis for tumor ablation with several types of cancer, as discussed in chapter 1.6.

Much work remains. A mathematical relationship between mRNA production and thermal dose does not guarantee a similar mathematical relationship exists with protein

production. This work used typical temperatures and duration of heat shocks for hyperthermia treatments. The relationship between thermal dose and mRNA production may not continue to exist as temperatures increase and durations shorten, both of which are commonly seen with ultrasonic surgery and any model will certainly need to incorporate cell viability. While the results in this study were statically significant, the standard deviations between experiments were often large. This might have been due to the limitations of rt-PCR and this researcher, but it also might indicate that any dose control model would not have the precision necessary for some gene therapies. Additionally, it seems likely that cell type and the particular therapeutic gene being used will also affect dose kinetics. Finally, several of the hsp70b promoted gene constructs tested thus far have used modified versions, such as adding additional HSEs to increase the amount of activation (Brade et al., 2000; Gerner et al., 2000; Luo et al., 2004; Vekris et al., 2000) which would also affect any predictive model.

Most importantly, clinically useful gene therapies that lend themselves to this particular modality of delivery and control will need to be found. Using ultrasonically-induced hyperthermia means that the area to be treated would be restricted in size with respect to reasonable treatment time constraints. The target area would also need to be somewhere that ultrasound can reach, limiting the depth of the treatment area from the skin or requiring more invasive protocols. A protocol that requires MRI-temperature mapping and precision ultrasonic hyperthermia also suggests that it would not be practical to require regular therapeutic gene activation over an extended time.

Given these constraints, the most practical use of this technique is like to be cancer treatments. Since cancer treatment is the goal of 65% of current research into gene therapy (Wirth et al., 2013), this is perhaps less of a limitation then it might seem. Gene therapy could be used as a replacement for or in conjunction with ultrasonic tumor ablation surgery. Several papers have examined the use of heat-induced "suicide" genes which cause apoptosis (Blackburn et al., 1998; Brade et al., 2000, 2003; Gerner et al., 2000; Lee et al., 2001).

It should be noted that many endogenous HSPs would also be activated with hyperthermia treatment, some of which have conflicting roles in cancer cells. These are referred to as "Janus-like properties" in a review by Calderwood and Ciocca in 2008 (Calderwood and Ciocca, 2008). HSPs evolved as a protective measure for cells and thus inhibit cell death and promote cellular repair. For example, while Hsp70b in particular is a non-functioning protein, the family of Hsp70 proteins inhibit cell death though caspase-dependent apoptosis pathways. For this reason HSPs are actually often overexpressed in cancer cells, possibly due to selection of cells over-expressing HSP in early tumor formation which prevent induced cell death during transformation. On the other hand, HSPs also play important roles in carrying tumor antigens and inflammatory agents, which can be exploited in tumor destruction and creating an immune response to metastases.

6 Appendices

6.1 Results from Chapter 3
Evaluating the Predictability of Hsp70b Activation Kinetics

All results are normalized to an unheated control.

Heat Shock 43°C 15 minutes

Time after Start of Heat Shock (hr)	Experiment 1	Experiment 2	Experiment 3
0	1.00	1.00	1.00
0.25	0.63	3.34	3.31
0.5	0.75	7.13	2.79
1	1.36	3.87	5.73
2	1.55	5.99	4.76
4	1.31	4.41	2.71

Heat Shock 43°C 30 minutes

Time after Start of Heat Shock (hr)	Experiment 1	Experiment 2	Experiment 3
0	1.00	1.00	1.00
0.25	1.19	2.44	2.11
0.5	5.17	14.81	6.08
1	9.08	13.51	9.34
2	25.70	17.38	12.00
4	1.83	1.35	2.37

Heat Shock 43°C 60 minutes

Time after Start of Heat Shock (hr)	Experiment 1	Experiment 2	Experiment 3
0	1.00	1.00	1.00
0.25	1.14	1.39	1.78
0.5	7.25	3.27	3.96
1	25.44	11.75	15.85
2	28.60	16.13	29.65
4	8.75	10.95	10.10

Heat Shock 44°C 15 minutes

Time after Start of Heat Shock (hr)	Experiment 1	Experiment 2	Experiment 3	Experiment 4
0	1.00	1.00	1.00	1.00
0.25	1.43	1.86	0.93	2.23
0.5	3.30	2.40	1.95	2.10
1	4.30	5.80	3.39	5.99
2	8.46	12.58	7.31	9.29
4	8.72	8.69	5.65	6.70
6		1.72	0.99	3.04

Heat Shock 44°C 30 minutes

Time after Start of Heat Shock (hr)	Experiment 1	Experiment 2	Experiment 3
0	1.00	1.00	1.00
0.25	1.93	3.82	2.64
0.5	7.06	8.80	1.26
1	17.14	25.57	1.72
2	22.97	35.77	7.83
4	15.59	25.76	8.55
6	4.90	5.10	2.75

Heat Shock 45°C 15 minutes

Time after Start of Heat Shock (hr)	Experiment 1	Experiment 2	Experiment 3
0	1.0	1.0	1.0
2	9.2	4.7	9.5
4	34.8	8.2	19.4
6	13.0	5.4	4.5
8	4.0	4.2	2.8
10	3.2	2.5	4.0
12	5.0	3.1	0.7

Heat Shock 45°C 30 minutes

Time after Start of Heat Shock (hr)	Experiment 1	Experiment 2	Experiment 3
0	1.00	1.00	1.00
4	20.20	21.20	27.44
8	14.85	24.82	17.22
12	7.56	10.07	5.49
16	2.94	4.90	2.77
20	1.78	2.69	1.55
24	1.28	1.46	1.12

6.2 Results from Chapter 4
Comparison of Hsp70b Kinetics in Two Heating Modalities

All results are normalized to an unheated control.

Heat Shock 43°C 15 minutes

Time after Heat Shock: 1 hr

	Ultrasound + HS	HS Alone
Pair 1	1.45	3.97
Pair 2	2.77	-
Pair 3	3.16	4.45
Pair 4	1.08	0.93

Time after Heat Shock: 2 hrs

	Ultrasound + HS	HS Alone
Pair 1	10.95	4.74
Pair 2	20.90	6.18
Pair 3	1.34	7.94

Time after Heat Shock: 4 hrs

	Ultrasound + HS	HS Alone
Pair 1	1.37	4.08
Pair 2	0.66	15.21
Pair 3	0.31	0.45
Pair 4	1.72	1.28
Pair 5	4.15	2.68

Heat Shock 44°C 15 minutes

Time after Heat Shock: 1 hr

	Ultrasound + HS	HS Alone
Pair 1	0.97	-
Pair 2	-	3.40
Pair 3	1.55	10.29
Pair 4	15.55	4.12

Time after Heat Shock: 2 hrs

	Ultrasound + HS	HS Alone
Pair 1	7.51	1.07
Pair 2	1.77	2.65
Pair 3	1.70	10.59

Time after Heat Shock: 4 hrs

	Ultrasound + HS	HS Alone
Pair 1	1.75	1.79
Pair 2	0.62	1.25
Pair 3	1.76	3.45
Pair 4	3.01	2.32
Pair 5	1.58	-

Time after Heat Shock: 6 hrs

	Ultrasound + HS	HS Alone
Pair 1	0.07	0.12
Pair 2	0.27	0.90
Pair 3	0.58	0.64

7 References

Acsadi, G., Dickson, G., Love, D.R., Jani, A., Walsh, F.S., Gurusinghe, A., Wolff, J.A., and Davies, K.E. (1991). Human dystrophin expression in mdx mice after intramuscular injection of DNA constructs. Nature *352*, 815–818.

Aiuti, A., Cattaneo, F., Galimberti, S., Benninghoff, U., Cassani, B., Callegaro, L., Scaramuzza, S., Andolfi, G., Mirolo, M., Brigida, I., et al. (2009). Gene therapy for immunodeficiency due to adenosine deaminase deficiency. N. Engl. J. Med. *360*, 447–458.

Alberts, B., Johnson, A., Lewis, J., Raff, M., Roberts, K., and Walter, P. (2002). Molecular Biology of the Cell (New York: Garland Science).

Alloway, J.L. (1932). The transformation in vitro of R pneumococci into S forms of different specific types by the use of filtered pneumococcus extracts. J. Exp. Med. *55*, 91–99.

Alloway, J.L. (1933). Further observations on the use of pneumococcus extracts in effecting transformation of type in vitro. J. Exp. Med. *57*, 265–278.

Andtbacka, R.H.I., Collichio, F.A., Amatruda, T., Senzer, N.N., Chesney, J., Delman, K.A., Spitler, L.E., Puzanov, I., Doleman, S., Ye, Y., et al. (2013). OPTiM: A randomized phase III trial of talimogene laherparepvec (T-VEC) versus subcutaneous (SC) granulocyte-macrophage colony-stimulating factor (GM-CSF) for the treatment (tx) of unresected stage IIIB/C and IV melanoma. J. Clin. Oncol. *31*.

Arai, Y., Kubo, T., Kobayashi, K., Ikeda, T., Takahashi, K., Takigawa, M., Imanishi, J., and Hirasawa, Y. (1999). Control of delivered gene expression in chondrocytes using heat shock protein 70B promoter. J. Rheumatol. *26*, 1769–1774.

Ardehali, A., Fyfe, A., Laks, H., Drinkwater, D.C., Jr, Qiao, J.H., and Lusis, A.J. (1995). Direct gene transfer into donor hearts at the time of harvest. J. Thorac. Cardiovasc. Surg. *109*, 716–719; discussion 719–720.

Arrhenius, S.A. (1889). Über die Dissociationswärme und den Einflusß der Temperatur auf den Dissociationsgrad der Elektrolyte. Z Phys. Chem *4*, 96–116.

Avery, O.T., Macleod, C.M., and McCarty, M. (1944). Studies on the Chemical Nature of the Substance Inducing Transformation of Pneumococcal Types: Induction of Transformation by a Deoxyribonucleic Acid Fraction Isolated from Pneumococcus Type III. J. Exp. Med. *79*, 137–158.

Barnett, S.B., and Kossoff, G.E. (1992). Symposium on Safety and Standardisation in Medical Ultrasound. Issues and Recommendations Regarding Thermal Mechanisms for Biological Effects of Ultrasound. Ultrasound Med. Biol. *18*, 731–810.

Barnett, S.B., ter Haar, G.R., Ziskin, M.C., Nyborg, W.L., Maeda, K., and Bang, J. (1994). Current status of research on biophysical effects of ultrasound. Ultrasound Med. Biol. *20*, 205–218.

Barnett, S.B., Rott, H.D., ter Haar, G.R., Ziskin, M.C., and Maeda, K. (1997). The sensitivity of biological tissue to ultrasound. Ultrasound Med. Biol. *23*, 805–812.

Blackburn, R.V., Galoforo, S.S., Corry, P.M., and Lee, Y.J. (1998). Adenoviral-mediated transfer of a heat-inducible double suicide gene into prostate carcinoma cells. Cancer Res. *58*, 1358–1362.

Blaese, R.M., Culver, K.W., Miller, A.D., Carter, C.S., Fleisher, T., Clerici, M., Shearer, G., Chang, L., Chiang, Y., Tolstoshev, P., et al. (1995). T lymphocyte-directed gene therapy for ADA- SCID: initial trial results after 4 years. Science *270*, 475–480.

Bordignon, C., Notarangelo, L.D., Nobili, N., Ferrari, G., Casorati, G., Panina, P., Mazzolari, E., Maggioni, D., Rossi, C., Servida, P., et al. (1995). Gene therapy in peripheral blood lymphocytes and bone marrow for ADA- immunodeficient patients. Science *270*, 470–475.

Borrelli, M.J., Schoenherr, D.M., Wong, A., Bernock, L.J., and Corry, P.M. (2001). Heat-activated transgene expression from adenovirus vectors infected into human prostate cancer cells. Cancer Res. *61*, 1113–1121.

Boztug, K., Schmidt, M., Schwarzer, A., Banerjee, P.P., Díez, I.A., Dewey, R.A., Böhm, M., Nowrouzi, A., Ball, C.R., Glimm, H., et al. (2010). Stem-cell gene therapy for the Wiskott-Aldrich syndrome. N. Engl. J. Med. *363*, 1918–1927.

Brade, A.M., Ngo, D., Szmitko, P., Li, P.X., Liu, F.F., and Klamut, H.J. (2000). Heat-directed gene targeting of adenoviral vectors to tumor cells. Cancer Gene Ther. *7*, 1566–1574.

Brade, A.M., Szmitko, P., Ngo, D., Liu, F.-F., and Klamut, H.J. (2003). Heat-directed suicide gene therapy for breast cancer. Cancer Gene Ther. *10*, 294–301.

Calderwood, S.K., and Ciocca, D.R. (2008). Heat shock proteins: stress proteins with Janus-like properties in cancer. Int. J. Hyperth. Off. J. Eur. Soc. Hyperthermic Oncol. North Am. Hyperth. Group *24*, 31–39.

Cavazzana-Calvo, M., Payen, E., Negre, O., Wang, G., Hehir, K., Fusil, F., Down, J., Denaro, M., Brady, T., Westerman, K., et al. (2010). Transfusion independence and HMGA2 activation after gene therapy of human β-thalassaemia. Nature *467*, 318–322.

Chung, A.H., Hynynen, K., Colucci, V., Oshio, K., Cline, H.E., and Jolesz, F.A. (1996). Optimization of spoiled gradient-echo phase imaging for in vivo localization of a focused ultrasound beam. Magn. Reson. Med. Off. J. Soc. Magn. Reson. Med. Soc. Magn. Reson. Med. *36*, 745–752.

Chung, A.H., Jolesz, F.A., and Hynynen, K. (1999). Thermal dosimetry of a focused ultrasound beam in vivo by magnetic resonance imaging. Med. Phys. *26*, 2017–2026.

Cideciyan, A.V., Hauswirth, W.W., Aleman, T.S., Kaushal, S., Schwartz, S.B., Boye, S.L., Windsor, E.A.M., Conlon, T.J., Sumaroka, A., Pang, J.-J., et al. (2009). Human RPE65 gene therapy for Leber congenital amaurosis: persistence of early visual improvements and safety at 1 year. Hum. Gene Ther. *20*, 999–1004.

Clement, G.T., White, J., and Hynynen, K. (2000). Investigation of a large-area phased array for focused ultrasound surgery through the skull. Phys. Med. Biol. *45*, 1071–1083.

Cline, H.E., Hynynen, K., Watkins, R.D., Adams, W.J., Schenck, J.F., Ettinger, R.H., Freund, W.R., Vetro, J.P., and Jolesz, F.A. (1995). Focused US system for MR imaging-guided tumor ablation. Radiology *194*, 731–737.

Cross, D., and Burmester, J.K. (2006). Gene Therapy for Cancer Treatment: Past, Present and Future. Clin. Med. Res. *4*, 218–227.

Culver, K.W. (1996). Gene Therapy: A Primer for Physicians (Mary Ann Liebert).

Damianou, C., and Hynynen, K. (1994). The effect of various physical parameters on the size and shape of necrosed tissue volume during ultrasound surgery. J. Acoust. Soc. Am. *95*, 1641–1649.

Daum, D.R., Buchanan, M.T., Fjield, T., and Hynynen, K. (1998). Design and evaluation of a feedback based phased array system for ultrasound surgery. IEEE Trans. Ultrason. Ferroelectr. Freq. Control *45*, 431–438.

Dawson, M.H., and Sia, R.H. (1931). In vitro transformations of pneumococcal types. I. A technique for inducing transformation of pneumococcal types in vitro. J. Exp. Med. *54*, 681–699.

Deckers, R., Quesson, B., Arsaut, J., Eimer, S., Couillaud, F., and Moonen, C.T.W. (2009). Image-guided, noninvasive, spatiotemporal control of gene expression. Proc. Natl. Acad. Sci. U. S. A. *106*, 1175–1180.

Deckers, R., Debeissat, C., Fortin, P.-Y., Moonen, C.T.W., and Couillaud, F. (2012). Arrhenius analysis of the relationship between hyperthermia and Hsp70 promoter activation: a comparison between ex vivo and in vivo data. Int. J. Hyperth. Off. J. Eur. Soc. Hyperthermic Oncol. North Am. Hyperth. Group *28*, 441–450.

Dewey, W.C. (2009). Arrhenius relationships from the molecule and cell to the clinic. Int. J. Hyperth. Off. J. Eur. Soc. Hyperthermic Oncol. North Am. Hyperth. Group *25*, 3–20.

Dewhirst, M.W., Viglianti, B.L., Lora-Michiels, M., Hanson, M., and Hoopes, P.J. (2003). Basic principles of thermal dosimetry and thermal thresholds for tissue damage from

hyperthermia. Int. J. Hyperth. Off. J. Eur. Soc. Hyperthermic Oncol. North Am. Hyperth. Group *19*, 267–294.

DiDomenico, B.J., Bugaisky, G.E., and Lindquist, S. (1982). Heat shock and recovery are mediated by different translational mechanisms. Proc. Natl. Acad. Sci. U. S. A. *79*, 6181–6185.

Duncan, R., and Hershey, J.W. (1984). Heat shock-induced translational alterations in HeLa cells. Initiation factor modifications and the inhibition of translation. J. Biol. Chem. *259*, 11882–11889.

Elias, W.J., Huss, D., Voss, T., Loomba, J., Khaled, M., Zadicario, E., Frysinger, R.C., Sperling, S.A., Wylie, S., Monteith, S.J., et al. (2013). A pilot study of focused ultrasound thalamotomy for essential tremor. N. Engl. J. Med. *369*, 640–648.

Eyring, H., and Stearn, A.E. (1939). The Application of the Theory of Absolute Reaction Rates to Proteins. Chem. Rev. *24*, 253–270.

Fernandes, M., Xiao, H., and Lis, J.T. (1994). Fine structure analyses of the Drosophila and Saccharomyces heat shock factor--heat shock element interactions. Nucleic Acids Res. *22*, 167–173.

Friedmann, T. (1992). A brief history of gene therapy. Nat. Genet. *2*, 93–98.

Fry, W.J., Mosberg, W.H., Jr, Barnard, J.W., and Fry, F.J. (1954). Production of focal destructive lesions in the central nervous system with ultrasound. J. Neurosurg. *11*, 471–478.

Gerner, E.W., Hersh, E.M., Pennington, M., Tsang, T.C., Harris, D., Vasanwala, F., and Brailey, J. (2000). Heat-inducible vectors for use in gene therapy. Int. J. Hyperth. Off. J. Eur. Soc. Hyperthermic Oncol. North Am. Hyperth. Group *16*, 171–181.

Gianfelice, D., Khiat, A., Amara, M., Belblidia, A., and Boulanger, Y. (2003). MR imaging-guided focused ultrasound surgery of breast cancer: correlation of dynamic contrast-enhanced MRI with histopathologic findings. Breast Cancer Res. Treat. *82*, 93–101.

Goss, S.A., Johnston, R.L., and Dunn, F. (1978). Comprehensive compilation of empirical ultrasonic properties of mammalian tissues. J. Acoust. Soc. Am. *64*, 423–457.

Guild, B.C., Finer, M.H., Housman, D.E., and Mulligan, R.C. (1988). Development of retrovirus vectors useful for expressing genes in cultured murine embryonal cells and hematopoietic cells in vivo. J. Virol. *62*, 3795–3801.

Gupta, R.S., and Singh, B. (1994). Phylogenetic analysis of 70 kD heat shock protein sequences suggests a chimeric origin for the eukaryotic cell nucleus. Curr. Biol. CB *4*, 1104–1114.

Hacein-Bey-Abina, S., Von Kalle, C., Schmidt, M., McCormack, M.P., Wulffraat, N., Leboulch, P., Lim, A., Osborne, C.S., Pawliuk, R., Morillon, E., et al. (2003). LMO2-associated clonal T cell proliferation in two patients after gene therapy for SCID-X1. Science *302*, 415–419.

Hacein-Bey-Abina, S., Hauer, J., Lim, A., Picard, C., Wang, G.P., Berry, C.C., Martinache, C., Rieux-Laucat, F., Latour, S., Belohradsky, B.H., et al. (2010). Efficacy of gene therapy for X-linked severe combined immunodeficiency. N. Engl. J. Med. *363*, 355–364.

Harvey, EN (1928). Further observations on the effect of high frequency sound waves on living matter. Biol. Bull. *55*, 459–469.

Hashemi, R.H., Bradley, W.G., and Lisanti, C.J. (2010). MRI: The Basics (Philadelphia, PA: LWW).

Hazle, J.D., Diederich, C.J., Kangasniemi, M., Price, R.E., Olsson, L.E., and Stafford, R.J. (2002). MRI-guided thermal therapy of transplanted tumors in the canine prostate using a directional transurethral ultrasound applicator. J. Magn. Reson. Imaging JMRI *15*, 409–417.

Henriques, F.C., and Moritz, A.R. (1947). Studies of Thermal Injury in the Conduction of Heat to and Through Skin and the Temperatures Attained Therein: A Theoretical and Experimental Investigation. Am. J. Pathol. *23*, 531–549.

Hershey, J.W., and Chase, M. (1952). Independent functions of viral protein and nucleic acid in growth of bacteriophage. J. Gen. Physiol. *36*, 39–56.

Hickman, M.A., Malone, R.W., Lehmann-Bruinsma, K., Sih, T.R., Knoell, D., Szoka, F.C., Walzem, R., Carlson, D.M., and Powell, J.S. (1994). Gene expression following direct injection of DNA into liver. Hum. Gene Ther. *5*, 1477–1483.

Hildebrandt, B., Wust, P., Ahlers, O., Dieing, A., Sreenivasa, G., Kerner, T., Felix, R., and Riess, H. (2002). The cellular and molecular basis of hyperthermia. Crit. Rev. Oncol. Hematol. *43*, 33–56.

Hill, C.R., Rivens, I., Vaughan, M.G., and ter Haar, G.R. (1994). Lesion development in focused ultrasound surgery: a general model. Ultrasound Med. Biol. *20*, 259–269.

Hindley, J., Gedroyc, W.M., Regan, L., Stewart, E., Tempany, C., Hynyen, K., Hynnen, K., Mcdannold, N., Macdanold, N., Inbar, Y., et al. (2004). MRI guidance of focused ultrasound therapy of uterine fibroids: early results. AJR Am. J. Roentgenol. *183*, 1713–1719.

Hindman, J. (1966). Proton resonance shift of water in the gas and liquid states. J Chem Phys *44*, 4582–4592.

Horvath, J. (1944). Ultraschallwirkung beim menschlichen Sarkom. Strahlentherapie *75*, 119–125.

Huang, Q., Hu, J.K., Lohr, F., Zhang, L., Braun, R., Lanzen, J., Little, J.B., Dewhirst, M.W., and Li, C.-Y. (2000). Heat-induced Gene Expression as a Novel Targeted Cancer Gene Therapy Strategy. Cancer Res. *60*, 3435–3439.

Hundt, W., O'Connell-Rodwell, C.E., Bednarski, M.D., Steinbach, S., and Guccione, S. (2007). In vitro effect of focused ultrasound or thermal stress on HSP70 expression and cell viability in three tumor cell lines. Acad. Radiol. *14*, 859–870.

Hunt, C., and Morimoto, R.I. (1985). Conserved features of eukaryotic hsp70 genes revealed by comparison with the nucleotide sequence of human hsp70. Proc. Natl. Acad. Sci. U. S. A. *82*, 6455–6459.

Hutchinson, E.B., and Hynynen, K. (1998). Intracavitary ultrasound phased arrays for prostate thermal therapies: MRI compatibility and in vivo testing. Med. Phys. *25*, 2392–2399.

Hynynen, K. (1993). Acoustic power calibrations of cylindrical intracavitary ultrasound hyperthermia applicators. Med. Phys. *20*, 129–134.

Hynynen, K., and Edwards, D.K. (1989). Temperature measurements during ultrasound hyperthermia. Med. Phys. *16*, 618–626.

Hynynen, K., Damianou, C.A., Colucci, V., Unger, E., Cline, H.H., and Jolesz, F.A. (1995). MR monitoring of focused ultrasonic surgery of renal cortex: experimental and simulation studies. J. Magn. Reson. Imaging JMRI *5*, 259–266.

Hynynen, K., Chung, A., Fjield, T., Buchanan, M., Daum, D., Colucci, V., Lopath, P., and Jolesz, F. (1996). Feasibility of using ultrasound phased arrays for MRI monitored noninvasive surgery. IEEE Trans. Ultrason. Ferroelectr. Freq. Control *43*, 1043–1053.

Hynynen, K., Clement, G.T., McDannold, N., Vykhodtseva, N., King, R., White, P.J., Vitek, S., and Jolesz, F.A. (2004). 500-element ultrasound phased array system for noninvasive focal surgery of the brain: a preliminary rabbit study with ex vivo human skulls. Magn. Reson. Med. Off. J. Soc. Magn. Reson. Med. Soc. Magn. Reson. Med. *52*, 100–107.

Hynynen, K., McDannold, N., Clement, G., Jolesz, F.A., Zadicario, E., Killiany, R., Moore, T., and Rosen, D. (2006). Pre-clinical testing of a phased array ultrasound system for MRI-guided noninvasive surgery of the brain--a primate study. Eur. J. Radiol. *59*, 149–156.

Illing, R.O., Kennedy, J.E., Wu, F., ter Haar, G.R., Protheroe, A.S., Friend, P.J., Gleeson, F.V., Cranston, D.W., Phillips, R.R., and Middleton, M.R. (2005). The safety and feasibility of extracorporeal high-intensity focused ultrasound (HIFU) for the

treatment of liver and kidney tumours in a Western population. Br. J. Cancer *93*, 890–895.

Ishihara, Y., Calderon, A., Watanabe, H., Okamoto, K., Suzuki, Y., Kuroda, K., and Suzuki, Y. (1995). A precise and fast temperature mapping using water proton chemical shift. Magn. Reson. Med. Off. J. Soc. Magn. Reson. Med. Soc. Magn. Reson. Med. *34*, 814–823.

Jacobson SG, Cideciyan AV, Ratnakaram R, and et al (2012). Gene therapy for leber congenital amaurosis caused by rpe65 mutations: Safety and efficacy in 15 children and adults followed up to 3 years. Arch. Ophthalmol. *130*, 9–24.

Jessup, M., Greenberg, B., Mancini, D., Cappola, T., Pauly, D.F., Jaski, B., Yaroshinsky, A., Zsebo, K.M., Dittrich, H., Hajjar, R.J., et al. (2011). Calcium Upregulation by Percutaneous Administration of Gene Therapy in Cardiac Disease (CUPID): a phase 2 trial of intracoronary gene therapy of sarcoplasmic reticulum Ca2+-ATPase in patients with advanced heart failure. Circulation *124*, 304–313.

Jolly, C., Usson, Y., and Morimoto, R.I. (1999). Rapid and reversible relocalization of heat shock factor 1 within seconds to nuclear stress granules. Proc. Natl. Acad. Sci. U. S. A. *96*, 6769–6774.

Kline, M.P., and Morimoto, R.I. (1997). Repression of the heat shock factor 1 transcriptional activation domain is modulated by constitutive phosphorylation. Mol. Cell. Biol. *17*, 2107–2115.

Kregel, K.C. (2002). Heat shock proteins: modifying factors in physiological stress responses and acquired thermotolerance. J. Appl. Physiol. Bethesda Md 1985 *92*, 2177–2186.

Kuroda, K. (2005). Non-invasive MR thermography using the water proton chemical shift. Int. J. Hyperth. Off. J. Eur. Soc. Hyperthermic Oncol. North Am. Hyperth. Group *21*, 547–560.

Lee, Y.J., Galoforo, S.S., Battle, P., Lee, H., Corry, P.M., and Jessup, J.M. (2001). Replicating adenoviral vector-mediated transfer of a heat-inducible double suicide gene for gene therapy. Cancer Gene Ther. *8*, 397–404.

Lehmann, J., and De Lateur, B. (1990). Therapeutic heat. In Therapeutic Heat and Cold, J. Lehmann, ed. (Baltimore: Williams & Wilkins).

Lewis, R. (2014). Gene Therapy's Second Act. Sci. Am. *310*.

Li, G.C., and Mak, J.Y. (1989). Re-induction of hsp70 synthesis: an assay for thermotolerance. Int. J. Hyperth. Off. J. Eur. Soc. Hyperthermic Oncol. North Am. Hyperth. Group *5*, 389–403.

Li, L.B., Chang, K.-H., Wang, P.-R., Hirata, R.K., Papayannopoulou, T., and Russell, D.W. (2012). Trisomy Correction in Down Syndrome Induced Pluripotent Stem Cells. Cell Stem Cell *11*, 615–619.

Lindquist, S., and Craig, E.A. (1988). The heat-shock proteins. Annu. Rev. Genet. *22*, 631–677.

Liu, Y., Kon, T., Li, C., and Zhong, P. (2005). High intensity focused ultrasound-induced gene activation in sublethally injured tumor cells in vitro. J. Acoust. Soc. Am. *118*, 3328–3336.

Liu, Y., Kon, T., Li, C., and Zhong, P. (2006). High intensity focused ultrasound-induced gene activation in solid tumors. J. Acoust. Soc. Am. *120*, 492–501.

Lizzi, F.L., and Ostromogilsky, M. (1987). Analytical modelling of ultrasonically induced tissue heating. Ultrasound Med. Biol. *13*, 607–618.

Locke, M., and Nussbaum, E. (2001). Continuous and pulsed ultrasound do not increase heat shock protein 72 content. Ultrasound Med. Biol. *27*, 1413–1419.

Lu, X., Sankin, G., Pua, E.C., Madden, J., and Zhong, P. (2009). Activation of transgene expression in skeletal muscle by focused ultrasound. Biochem. Biophys. Res. Commun. *379*, 428–433.

Luo, P., He, X., Tsang, T.C., and Harris, D.T. (2004). A novel inducible amplifier expression vector for high and controlled gene expression. Int. J. Mol. Med. *13*, 319–325.

Madsen, E.L., Frank, G.R., and Dong, F. (1998). Liquid or solid ultrasonically tissue-mimicking materials with very low scatter. Ultrasound Med. Biol. *24*, 535–542.

Manthorpe, M., Cornefert-Jensen, F., Hartikka, J., Felgner, J., Rundell, A., Margalith, M., and Dwarki, V. (1993). Gene therapy by intramuscular injection of plasmid DNA: studies on firefly luciferase gene expression in mice. Hum. Gene Ther. *4*, 419–431.

McDannold, Hynynen, K., Wolf, D., Wolf, G., and Jolesz, F. (1998). MRI evaluation of thermal ablation of tumors with focused ultrasound. J. Magn. Reson. Imaging JMRI *8*, 91–100.

McTaggart, S., and Al-Rubeai, M. (2002). Retroviral vectors for human gene delivery. Biotechnol. Adv. *20*, 1–31.

Miller, A.D. (1992). Retroviral vectors. Curr. Top. Microbiol. Immunol. *158*, 1–24.

Miller, A.D., Miller, D.G., Garcia, J.V., and Lynch, C.M. (1993). Use of retroviral vectors for gene transfer and expression. Methods Enzymol. *217*, 581–599.

Mir, L.M., Banoun, H., and Paoletti, C. (1988). Introduction of definite amounts of nonpermeant molecules into living cells after electropermeabilization: direct access to the cytosol. Exp. Cell Res. *175*, 15–25.

Mizzen, L.A., and Welch, W.J. (1988). Characterization of the thermotolerant cell. I. Effects on protein synthesis activity and the regulation of heat-shock protein 70 expression. J. Cell Biol. *106*, 1105–1116.

Moonen, C.T.W. (2007). Spatio-temporal control of gene expression and cancer treatment using magnetic resonance imaging-guided focused ultrasound. Clin. Cancer Res. Off. J. Am. Assoc. Cancer Res. *13*, 3482–3489.

Nakai, H., Montini, E., Fuess, S., Storm, T.A., Grompe, M., and Kay, M.A. (2003). AAV serotype 2 vectors preferentially integrate into active genes in mice. Nat. Genet. *34*, 297–302.

Nussbaum, E.L., and Locke, M. (2007). Heat shock protein expression in rat skeletal muscle after repeated applications of pulsed and continuous ultrasound. Arch. Phys. Med. Rehabil. *88*, 785–790.

De Poorter, J., De Wagter, C., De Deene, Y., Thomsen, C., Ståhlberg, F., and Achten, E. (1995). Noninvasive MRI thermometry with the proton resonance frequency (PRF) method: in vivo results in human muscle. Magn. Reson. Med. Off. J. Soc. Magn. Reson. Med. Soc. Magn. Reson. Med. *33*, 74–81.

Quesson, B., de Zwart, J.A., and Moonen, C.T. (2000). Magnetic resonance temperature imaging for guidance of thermotherapy. J. Magn. Reson. Imaging JMRI *12*, 525–533.

Rhoads, R.E., and Lamphear, B.J. (1995). Cap-independent translation of heat shock messenger RNAs. Curr. Top. Microbiol. Immunol. *203*, 131–153.

Rieke, V., Kinsey, A.M., Ross, A.B., Nau, W.H., Diederich, C.J., Sommer, G., and Pauly, K.B. (2007). Referenceless MR thermometry for monitoring thermal ablation in the prostate. IEEE Trans. Med. Imaging *26*, 813–821.

Ripert, T., Azémar, M.-D., Ménard, J., Bayoud, Y., Messaoudi, R., Duval, F., and Staerman, F. (2010). Transrectal high-intensity focused ultrasound (HIFU) treatment of localized prostate cancer: review of technical incidents and morbidity after 5 years of use. Prostate Cancer Prostatic Dis. *13*, 132–137.

Ritossa, F. (1962). A new puffing pattern induced by temperature shock and DNP in drosophila. Experientia *18*, 571–573.

Rivière, I., Brose, K., and Mulligan, R.C. (1995). Effects of retroviral vector design on expression of human adenosine deaminase in murine bone marrow transplant recipients engrafted with genetically modified cells. Proc. Natl. Acad. Sci. U. S. A. *92*, 6733–6737.

Robbins, P.D., and Ghivizzani, S.C. (1998). Viral vectors for gene therapy. Pharmacol. Ther. *80*, 35–47.

Rogers, S., Lowenthal, A., Terheggen, H.G., and Columbo, J.P. (1973). Induction of arginase activity with the Shope papilloma virus in tissue culture cells from an argininemic patient. J. Exp. Med. *137*, 1091–1096.

Romano, G. (2012). Development of safer gene delivery systems to minimize the risk of insertional mutagenesis-related malignancies: a critical issue for the field of gene therapy. ISRN Oncol. *2012*, 616310.

Rome, C., Couillaud, F., and Moonen, C.T.W. (2005). Spatial and temporal control of expression of therapeutic genes using heat shock protein promoters. Methods San Diego Calif *35*, 188–198.

Rosenberg, S.A., Anderson, W.F., Blaese, M., Hwu, P., Yannelli, J.R., Yang, J.C., Topalian, S.L., Schwartzentruber, D.J., Weber, J.S., and Ettinghausen, S.E. (1993). The development of gene therapy for the treatment of cancer. Ann. Surg. *218*, 455–463; discussion 463–464.

Rylander, M.N., Feng, Y., Zhang, Y., Bass, J., Jason Stafford, R., Volgin, A., Hazle, J.D., and Diller, K.R. (2006). Optimizing heat shock protein expression induced by prostate cancer laser therapy through predictive computational models. J. Biomed. Opt. *11*, 041113.

Rylander, M.N., Feng, Y., Zimmermann, K., and Diller, K.R. (2010). Measurement and mathematical modeling of thermally induced injury and heat shock protein expression kinetics in normal and cancerous prostate cells. Int. J. Hyperth. Off. J. Eur. Soc. Hyperthermic Oncol. North Am. Hyperth. Group *26*, 748–764.

Sadoshima, J., Jahn, L., Takahashi, T., Kulik, T.J., and Izumo, S. (1992). Molecular characterization of the stretch-induced adaptation of cultured cardiac cells. An in vitro model of load-induced cardiac hypertrophy. J. Biol. Chem. *267*, 10551–10560.

Sambrook, J., Westphal, H., Srinivasan, P.R., and Dulbecco, R. (1968). The integrated state of viral DNA in SV40-transformed cells. Proc. Natl. Acad. Sci. U. S. A. *60*, 1288–1295.

Samulski, T.V., MacFall, J., Zhang, Y., Grant, W., and Charles, C. (1992). Non-invasive thermometry using magnetic resonance diffusion imaging: potential for application in hyperthermic oncology. Int. J. Hyperth. Off. J. Eur. Soc. Hyperthermic Oncol. North Am. Hyperth. Group *8*, 819–829.

Sapareto, S.A., and Dewey, W.C. (1984). Thermal dose determination in cancer therapy. Int. J. Radiat. Oncol. Biol. Phys. *10*, 787–800.

Schwartz, B., Benoist, C., Abdallah, B., Rangara, R., Hassan, A., Scherman, D., and Demeneix, B.A. (1996). Gene transfer by naked DNA into adult mouse brain. Gene Ther. *3*, 405–411.

Sikes, M.L., O'Malley, B.W., Jr, Finegold, M.J., and Ledley, F.D. (1994). In vivo gene transfer into rabbit thyroid follicular cells by direct DNA injection. Hum. Gene Ther. *5*, 837–844.

Silcox, C.E., Smith, R.C., King, R., McDannold, N., Bromley, P., Walsh, K., and Hynynen, K. (2005). MRI-guided ultrasonic heating allows spatial control of exogenous luciferase in canine prostate. Ultrasound Med. Biol. *31*, 965–970.

Smith, R.C., Machluf, M., Bromley, P., Atala, A., and Walsh, K. (2002). Spatial and temporal control of transgene expression through ultrasound-mediated induction of the heat shock protein 70B promoter in vivo. Hum. Gene Ther. *13*, 697–706.

Stepanow B, Huber P, Brix G, Debus J, Bader R, van Kaick G, and Lorenz WJ (1995). Fast MRI temperature monitoring: application in focused ultrasound therapy of malignant tissue in vivo. Proc SMR 3rd Meeting, ISSN 1065–9889 2:1172.

Stolberg, S.G. (1999). The biotech death of Jesse Gelsinger. N. Y. Times Mag. 136–140, 149–150.

Szybalska, E.H., and Szybalska, W. (1962). Genetics of human cess line. IV. DNA-mediated heritable transformation of a biochemical trait. Proc. Natl. Acad. Sci. U. S. A. *48*, 2026–2034.

Tang, D., Khaleque, M.A., Jones, E.L., Theriault, J.R., Li, C., Wong, W.H., Stevenson, M.A., and Calderwood, S.K. (2005). Expression of heat shock proteins and heat shock protein messenger ribonucleic acid in human prostate carcinoma in vitro and in tumors in vivo. Cell Stress Chaperones *10*, 46–58.

Tang, H., Liu, Y., Madabusi, L., and Gilmour, D.S. (2000). Promoter-proximal pausing on the hsp70 promoter in Drosophila melanogaster depends on the upstream regulator. Mol. Cell. Biol. *20*, 2569–2580.

Tempany, C.M.C., Stewart, E.A., McDannold, N., Quade, B.J., Jolesz, F.A., and Hynynen, K. (2003). MR imaging-guided focused ultrasound surgery of uterine leiomyomas: a feasibility study. Radiology *226*, 897–905.

Terheggen, H.G., Lowenthal, A., Lavinha, F., Colombo, J.P., and Rogers, S. (1975). Unsuccessful trial of gene replacement in arginase deficiency. Z. Für Kinderheilkd. *119*, 1–3.

Thomas, J.L., Wu, F., and Fink, M. (1996). Time reversal focusing applied to lithotripsy. Ultrason. Imaging *18*, 106–121.

Vekris, A., Maurange, C., Moonen, C., Mazurier, F., De Verneuil, H., Canioni, P., and Voisin, P. (2000). Control of transgene expression using local hyperthermia in combination with a heat-sensitive promoter. J. Gene Med. *2*, 89–96.

Voellmy, R. (1994). Transduction of the stress signal and mechanisms of transcriptional regulation of heat shock/stress protein gene expression in higher eukaryotes. Crit. Rev. Eukaryot. Gene Expr. *4*, 357–401.

Volpers, C., and Kochanek, S. (2004). Adenoviral vectors for gene transfer and therapy. J. Gene Med. *6 Suppl 1*, S164–171.

Westphal, M., Ylä-Herttuala, S., Martin, J., Warnke, P., Menei, P., Eckland, D., Kinley, J., Kay, R., and Ram, Z. (2013). Adenovirus-mediated gene therapy with sitimagene ceradenovec followed by intravenous ganciclovir for patients with operable high-grade glioma (ASPECT): a randomised, open-label, phase 3 trial. Lancet Oncol. *14*, 823–833.

Wirth, T., Samaranayake, H., Pikkarainen, J., Määttä, A.-M., and Ylä-Herttuala, S. (2009). Clinical trials for glioblastoma multiforme using adenoviral vectors. Curr. Opin. Mol. Ther. *11*, 485–492.

Wirth, T., Parker, N., and Ylä-Herttuala, S. (2013). History of gene therapy. Gene *525*, 162–169.

Wolff, J.A., Malone, R.W., Williams, P., Chong, W., Acsadi, G., Jani, A., and Felgner, P.L. (1990). Direct gene transfer into mouse muscle in vivo. Science *247*, 1465–1468.

Wood, RW, and Loomis, AL (1927). The physical and biological effects of high frequency sound waves of greater intensity. Lond. Edinb. Dublin Philos. Mag. J. Sci. *4*, 417–436.

Worgall, S. (2005). A realistic chance for gene therapy in the near future. Pediatr. Nephrol. Berl. Ger. *20*, 118–124.

Xu, Q., Schett, G., Li, C., Hu, Y., and Wick, G. (2000). Mechanical stress-induced heat shock protein 70 expression in vascular smooth muscle cells is regulated by Rac and Ras small G proteins but not mitogen-activated protein kinases. Circ. Res. *86*, 1122–1128.

Yang, Y., and Wilson, J.M. (1995). Clearance of adenovirus-infected hepatocytes by MHC class I-restricted CD4+ CTLs in vivo. J. Immunol. Baltim. Md 1950 *155*, 2564–2570.

Yang, Y., Su, Q., and Wilson, J.M. (1996). Role of viral antigens in destructive cellular immune responses to adenovirus vector-transduced cells in mouse lungs. J. Virol. *70*, 7209–7212.

Ylä-Herttuala, S. (2012). Endgame: glybera finally recommended for approval as the first gene therapy drug in the European union. Mol. Ther. J. Am. Soc. Gene Ther. *20*, 1831–1832.

Yoo, J.J., Soker, S., Lin, L.F., Mehegan, K., Guthrie, P.D., and Atala, A. (1999). Direct in vivo gene transfer to urological organs. J. Urol. *162*, 1115–1118.

Yueh, A., and Schneider, R.J. (2000). Translation by ribosome shunting on adenovirus and hsp70 mRNAs facilitated by complementarity to 18S rRNA. Genes Dev. *14*, 414–421.

Zhang, Y., and Friedlander, R.M. (2011). Using non-coding small RNAs to develop therapies for Huntington's disease. Gene Ther. *18*, 1139–1149.

Zhang, J., Kuhlenschmidt, M.S., and Dunn, F. (1991). Influences of structural factors of biological media on the acoustic nonlinearity parameter B/A. J. Acoust. Soc. Am. *89*, 80–91.

Zinder, N.D., and Lederberg, J. (1952). Genetic exchange in Salmonella. J. Bacteriol. *64*, 679–699.

Zippel, D.B., and Papa, M.Z. (2005). The use of MR imaging guided focused ultrasound in breast cancer patients; a preliminary phase one study and review. Breast Cancer Tokyo Jpn. *12*, 32–38.